IDENTIFYING AND CHARACTERIZING NOVEL MECHANISMS IN THE ESTABLISHMENT AND MAINTENANCE OF SYNAPSES IN *DROSOPHILA*

by

MICHAEL ALBERT SPINNER

A DISSERTATION

Presented to the Department of Chemistry and Biochemistry
and the Graduate School of the University of Oregon
in partial fulfillment of the requirements
for the degree of
Doctor of Philosophy

June 2018

DISSERTATION APPROVAL PAGE

Student: Michael Albert Spinner

Title: Identifying and Characterizing Novel Mechanisms in the Establishment and Maintenance of Synapses in *Drosophila*

This dissertation has been accepted and approved in partial fulfillment of the requirements for the Doctor of Philosophy degree in the Department of Chemistry and Biochemistry by:

Dr. Ken Prehoda	Chairperson
Dr. Tory Herman	Advisor
Dr. Chris Doe	Core Member
Dr. Tom Stevens	Core Member
Dr. Phil Washbourne	Institutional Representative

and

Sara D. Hodges	Interim Vice Provost and Dean of the Graduate School

Original approval signatures are on file with the University of Oregon Graduate School.

Degree awarded June 2018

DISSERTATION ABSTRACT

Michael Albert Spinner

Doctor of Philosophy

Department of Chemistry and Biochemistry

June 2018

Title: Identifying and Characterizing Novel Mechanisms in the Establishment and Maintenance of Synapses in *Drosophila*

Synapse development is a stepwise process that requires the recruitment of key synaptic components to active zones, followed by continual maintenance of these structures to maintain connectivity and stability throughout the life of the organisms. Early synapse development requires the recruitment of early scaffolding proteins to establish stable connectivity as well as provide sites of recruitment of other vital synaptic proteins. One of the earliest proteins to be localized to the synapse is the conserved protein Syd-1. Syd-1 proteins contain a Rho GTPase activating protein (GAP)-like domain of unclear significance. Here I show that *Drosophila* Syd-1 interacts with all six fly Rhos and has GAP activity towards RAC1. I then show that lacks GAP activity localizes normally to presynaptic sites and is sufficient to recruit Nrx-1 but fails to cluster Brp normally and genetically interacts with RAC1 in vivo. I conclude that contrary to previous models, the GAP domain of fly Syd-1 is active and required for presynaptic development.

Additionally, I've identified a previously uncharacterized protein, Vezl, as being critical for retrograde axonal transport and synaptic maintenance. I found that Vezl required for normal neuronal growth and that *vezl* loss resulted in decreased

neuron size and the formation of swollen neuronal terminals that accumulated membrane markers and axonal transport cargo. I found that *vezl* mutants specifically retrograde transport of cargo and particularly affected signaling endosomes. The signaling endosomes were unable to initiate retrograde transport in *vezl* mutants and remained stuck within the distal boutons unable to relay their signaling peptides back to the nucleus. I conclude that Vezl is serving a role in attaching retrograde cargo to dynein and the microtubules specifically at neuron tips so that they can undergo retrograde axonal transport.

This dissertation includes previously published co-authored material.

CURRICULUM VITAE

NAME OF AUTHOR: Michael Albert Spinner

GRADUATE AND UNDERGRADUATE SCHOOLS ATTENDED:

University of Oregon, Eugene

University of Idaho, Moscow

DEGREES AWARDED:

Doctor of Philosophy, Chemistry, 2018, University of Oregon
Bachelor of Science, Chemistry and Biochemistry, 2011, University of Idaho

AREAS OF SPECIAL INTEREST:

Molecular, Cellular and Developmental Biology

Developmental Neuroscience

PROFESSIONAL EXPERIENCE:

Graduate Teaching Fellow, Department of Chemistry, University of Oregon, 2011-2012, 2017

Research Assistant, Dr. Ray von Wandruszka, University of Idaho, 2009-2011

Environmental Technician, Idaho Department of Environmental Quality, 2007-2009

GRANTS, AWARDS, AND HONORS:

Biochemistry and Biophysics Training Grant, National Institute of Health, 2013- 2016

Outstanding Undergraduate Research Award, University of Idaho, 2011

Dean's Award for Excellence, University of Idaho, 2011

PUBLICATIONS:

Spinner, M.A., Walla, D., and Herman, T.G. 2017. *Drosophila* Syd-1 has RhoGAP activity that is required for presynaptic clustering of Bruchpilot/ELKS but not Neurexin-1. *Genetics* 208: 705-716

Pollard, M., Spinner, M.A. and Wandruszka, R. 2013. Construction and evaluation of a fluorescent sensor for the detection of high explosives. *Anal. Lett..* 46: 266-274

ACKNOWLEDGMENTS

I would like to sincerely thank my advisor, Dr. Tory Herman, for her mentorship and guidance during my time in her lab. I joined her lab with no previous knowledge in the field, and it was her skill, patience and guidance that allowed me to explore new areas of research and set me up to succeed. It was through my interactions in her lab that allowed me develop an interest in a new field and pursue a future career in science. I thank all the former Herman lab members for vital feedback and technical support, and various undergrads, summer students and graduate rotation students that have I have had the pleasure of working with along the way. I greatly appreciate the advice and feedback from my dissertation committee members: doctors Ken Prehoda, Chris Doe, Tom Stevens and Phil Westbourne and the tools and resource they and their labs provided as my research took new and interesting turns. I am grateful to the Institute of Molecular Biology and the colleagues and friends, past and present, therein. It's been fun.

Finally I'd like to thank my family. It was my parent's, George and Nancy Spinner, whose early support and patience encouraged a passion in science and allowed the freedom to explore the world through different avenues. I'd also like to thank my two older brothers, Adam and Justin Spinner. They didn't help, but they did keep me level headed and focused through the process.

I'd also like to thank the Biochemistry and Biophysics training grant and the National Institute of Health who provided funding for my projects.

TABLE OF CONTENTS

Chapter Page

I. INTRODUCTION 1

II. *DROSOPHILA* SYD-1 HAS RHOGAP ACTIVITY THAT IS REQUIRED FOR PRESYNAPTIC CLUSTERING OF BRUCHPILOT/ELKS BUT NOT NEUREXIN-1 4

Journal Style Information 4

Author Contributions 4

Introduction 4

Materials and Methods 6

Results 12

Drosophila Syd-1 Interacts With All Six Rho GTPases, and its Predicted GAP Domain Enhances the GTPase Activities of Rac1 and CDC42 12

Decreasing syd-1 Dosage Impairs the Ability of Wild-type but Not Constituitively-active Rac1 to Increase NMJ Bouton Number 13

Overexpression of Wild-type or R979A Mutant Syd-1 in Wild-type Motorneurons Causes Similar Increases in NMJ Bouton Number and Nrx-1 Levels 16

Unlike Wild-type Syd-1, R979A Mutant Syd-1 Does Not Rescue the Decrease in NMJ Bouton Number in *syd-1* Mutants, Despite Restoring Nrx-1 Levels 17

Syd-1's RhoGAP Activity Is Required For Normal Brp Clustering, As Is the RacGEF Trio 19

Syd-1 Is Required for Rac^{V12} to Increase Nrx-1 Levels 20

Discussion 21

The Role of Syd-1's GAP Activity in Clustering Brp 21

The Roles of Rac1 and Syd-1 in Recruiting Nrx-1 24

Fly Syd-1 Compared with Worm Syd-1 and Mouse mSYD1A 24

Bridge to Chapter III 26

III. IDENTIFITICATION OF VEZATIN-LIKE, A NOVEL GENE REQUIRED FOR AXONAL TRANSPORT 37

Introduction 37

Materials and Methods 39

Results 41

Vezatin-like (Vezl) is Required for Normal Photoreceptor Axon Terminal Morphology 41

Loss of Vezl Results in Defects in NMJ Development and Distal Bouton Morphology 42

Vezl Promotes NMJ Growth, Localizes to Microtubules, and is Enriched in Distal Boutons 43

vezl Mutants Have Normal Synaptic Vesicle Distribution, but Excessive Endosome Accumulation 44

Retrograde BMP Signaling is Affected by Vezl Loss 46

Defects in Axonal Transport of Motor Neuron Axons 47

Defects in Axonal Transport at Boutons 49

Loss of Vezl Does Not Affect Microtubule Formation in NMJs 50

Human Vezatin is Unable to Rescue Loss of Vezl in Flies 51

Future Experiments 52

Discussion 52

Fly Vezatin-like As a Homologue to Vertebrate Vezatin 52

Model for Vezatin's Role in Retrograde Axonal Transport 53

Vezatin's Role in BMP Signaling 55

IV. CONCLUSIONS 56

APPENDIX: SUPPLEMENTAL MATERIAL (CHAPTER II) 68

REFERENCES CITED 71

LIST OF FIGURES

Figure Page

CHAPTER II

1. *Drsophila* Syd-1 interacts with all six RhoGTPases. Its predicted GAP domain enhances the GTPase activities of Rac1 and CDC42 27

2. Wild-type Rac1, unlike Rac^{v12}, requires wild-type Syd-1 levels to promote NMJ growth 28

3. Wild-type and R979A mutant Syd-1 colocalize with Brp and cause similar increases in NMJ bouton number and Nrx-1 levels 30

4. The decrease in NMJ bouton number in *syd-1* mutants is fully recued by wild-type Syd-1 but unaltered by R979A mutant Syd-1 32

5. Both wild-type and R979A mutant Syd-1 fully restore NMJ Nrx-1 levels in *syd-1* mutants 34

6. The defects in Brp clustering in *syd-1* mutants is fully rescued by wild-type, but notR979A mutant Syd-1 35

7. Rac^{V12} requires Syd-1 in order to increase Nrx-1 levels at NMJ 36

CHAPTER III

1. CG7705/Vezatin-like (Vezl) is required for normal photoreceptor axon terminal morphology 58

2. Loss of Vezl results in defects in larval neuromuscular junction development and distal bouton morphology 59

3. Vezl promotes NMJ development, localizes along axons and is enriched in distal boutons 60

4. Distal NMJ boutons in *vezl* mutants have normal-looking synaptic vesicle distribution but abnormal dense corve vesicles and endosomes 61

5. Retrograde BMP signaling is affected in *vezl* mutants 63

6. Dense core vesicle transport is disrupted in *vezl* mutants 64

Figure Page

7. Transport of BMP signaling molecules are also disrupted in *vezl* mutants 65

8. Retrograde transport of endosomes is disrupted in the distal bouton of *vezl* mutants 66

9. Expression of a human Vezatin (hVez) transgene is unable to properly localize and cannot rescue loss of *vezl*. 67

CHAPTER I

INTRODUCTION

Preface

The nervous system is a large, sprawling network of cells that that coordinate and influence the activity of all higher organisms. The primary constituent in the nervous system is the neuron, a specialized cell that converts electrical signals into chemical signals that can be relayed throughout the organism. The nervous systems ability to do so is predicated on neuron sending out a long process, the axon, to navigate and identify its correct partner and form specialized connections with them called synapses. Altogether the individual interlocking components of the nervous system come together to serve its diverse roles and complex function. However, while the field of neuroscience is ever advancing and great strides are being made in understanding how neurons function in relation to cognition, behavior and disease, there is still a large amount of information that is unknown about their basic cellular functions.

In order to simplify he mystery of it's molecular and cellular function, we can break down the nervous system into it's individual cells, identify and characterize the key proteins required within those cells and then use that information to understand how they function in context to the whole nervous system. Forward genetic screens in model organisms have become a powerful means of identifying the proteins

responsible for carrying out critical cellular process. In systems that are poorly understood or lacking aspects of function, they prove to be particularly insightful in identifying new and previously uncharacterized components. My thesis addresses two genes that have been found to be required for early synapse development: Syd-1, which is required for synapse assembly, and Vezatin-like, which is required for retrograde axonal transport. Chapter II of this thesis contains previously published coauthored material and includes data obtained by myself and from a former lab member David Walla.

Synapse assembly and active zone establishment

The neuron is a unique cell that's structurally asymmetric; extending long axons away from the cell body that can cover large distances. The process of synapse formation occurs upon the axon of a neuron reaching its target cell and stabilizing its cell-cell junction. This process occurs in stages through the sequential recruitment and localization of several key synaptic proteins. Some of the earliest proteins localized to developing synapses are scaffolding proteins (Torres et al. 2017); proteins that are localized to synapses and recruit and localize other synaptic proteins to establish active zones; specialized regions of the presynapse where synaptic vesicles are bound, primed and released through the synaptic cleft (Maritzen and Haucke 2018). This process must be timely and spatially regulated so that neurotransmitter release occurs directly opposed to postsynaptic receptors. Active zone proteins maintain this structural and functional integrity during the lifespan of the neuron and are able to undergo molecular remodeling to support the requirements of synaptic activity and plasticity (Torrese et al. 2017).

Most active zone proteins are conserved between vertebrates and invertebrates. These include Rab3-interacting molecules (RIMs), RIM-binding proteins, ElKS/BRP, Liprin-α, Nuerexin and Syd-1. These proteins are all expressed at high levels during development and persist in adult brain, indicating a permanent and crucial role for active zone proteins in synapse function (Maritzen and Haucke 2018). While the identity of scaffolding proteins have largely been identified the mechanisms underlying their ability to establish and promote synapse development is still largely unknown.

Axonal transport and synaptic maintenance

Once established, synapses must be maintained for the life of the neuron. This is in large part dependent on axonal transport, which circulates synaptic vesicles and proteins to maintain homeostasis and is required for the relay of signals for cell survival and growth pathways (Cioni et al. 2018). Axonal transport requires molecular motors to move cargoes along microtubules tracts; kinesins that primarily undergo anterograde transport and dyneins that primarily undergo retrograde transport. In order to function properly and maintain neuronal integrity, molecular motors most be in place and of sufficient number, all of the infrastructure including actin and microtubules must be in established, and cargo adaptor proteins must be present to attach the proper cargo to the motors. The mechanisms that regulate axonal transport are not well understood, but have gained interest as of late with preliminary evidence showing axonal transport and trafficking being negatively affect in neurodegenerative diseases such as Huntington's, Alzheimer's, and Parkinson's disease (Perlson, et al. 2010).

CHAPTER II

DROSOPHILA SYD-1 HAS RHOGAP ACTIVITY THAT IS REQUIRED FOR PRESYNAPTIC CLUSTERING OF BRUCHPILOT/ELKS BUT NOT NEUREXIN-1

JOURNAL STYLE INFORMATION

AUTHOR CONTRIBUTIONS

I performed the experiments presented in this manuscript, with the exception of Fig. 1. This data was obtained and analyzed by a former graduate student, David Walla. Dr. Herman, Dr. Walla and I designed the experiments and wrote the manuscript together.

INTRODUCTION

The assembly of synaptic connections between neurons and their targets is initiated by cell–cell adhesion and culminates in the clustering of presynaptic and postsynaptic components at apposing sites (Melom and Littleton 2011; Chia *et al.* 2013). Forward genetic screens in worm and fly have identified the presynaptic cytosolic protein Syd-1 as a critical regulator of presynaptic assembly (Hallam *et al.* 2002; Owald *et al.* 2010; Holbrook *et al.* 2012). In both species, Syd-1 is among

the first proteins to arrive at nascent presynaptic sites and is required for the subsequent recruitment of multiple presynaptic components, including scaffolding proteins, active zone (AZ) proteins, synaptic vesicles (SVs), and mitochondria (Hallam *et al.* 2002; Dai *et al.* 2006; Patel *et al.*2006; Owald *et al.* 2010, 2012; Holbrook *et al.* 2012). Fly Syd-1 has been shown to directly bind and cluster the AZ ELKS family protein Bruchpilot (Brp; Owald *et al.* 2010) and the presynaptic adhesion molecule Neurexin (Nrx-1; Owald *et al.* 2012); presynaptic loss of fly Syd-1 disrupts Brp and Nrx-1 localization within neuromuscular junction (NMJ) boutons, decreasing the number of boutons that form (Owald *et al.* 2010, 2012). More recently, a mouse Syd-1 ortholog, mSYD1A, was identified and shown to be required for the localization of SVs to presynaptic sites (Wentzel *et al.* 2013), suggesting that at least some aspects of Syd-1 function are conserved between invertebrates and vertebrates.

Syd-1 proteins in both invertebrates and vertebrates contain a Rho GTPase activating protein (GAP)-like domain; however, the importance of this domain to the ability of Syd-1 to promote presynaptic development is unclear. Classically, RhoGAPs increase the GTPase activity of one or more Rho family proteins—Rac, Rho, and Cdc42—accelerating their switch from an active, GTP-bound state to a conformationally distinct inactive, GDP-bound state (Scheffzek and Ahmadian 2005; Tcherkezian and Lamarche-Vane 2007). Rho GTPases are also regulated by guanine exchange factors (GEFs) that accelerate their switch back from the GDP- to the GTP-bound state (Rossman *et al.* 2005). Rho GTPases and their regulators have

been implicated in multiple aspects of neural development, including presynaptic assembly, but the molecular mechanism(s) by which they regulate the latter are unknown (Ball *et al.* 2010; Nahm *et al.* 2010; Tolias *et al.* 2011). The RhoGAP domains of the worm and fly Syd-1 proteins lack key conserved amino acids and so have been thought to lack GAP activity (Hallam *et al.* 2002; Wentzel *et al.* 2013); indeed, while worm Syd-1 was recently found to bind GTP-bound MIG-2/Rac, no GAP activity has ever been detected (Hallam *et al.* 2002; Xu *et al.* 2015). By contrast, mouse mSYD1A does have GAP activity toward RhoA (Wentzel *et al.* 2013), but whether this activity is required for mSYD1A function is not clear. Mutant forms of mSYD1A that lack the RhoGAP domain are sufficient to cluster SVs at presynaptic sites in cultured neurons, but their ability to rescue the SV docking defect in *mSYD1A*^{KO}mutant mice has not been tested, and the mouse genome contains a second Syd-1 homolog (Wentzel *et al.* 2013), whose presence complicates the interpretation of these experiments (see *Discussion*).

Here, we show that, contrary to previous evidence (Wentzel *et al.* 2013), fly Syd-1 does have RhoGAP activity. We use a mutant form of Syd-1 that specifically lacks GAP activity to show that Syd-1 has both GAP-dependent and GAP-independent functions in presynaptic assembly. And, finally, we identify Rac1 as a Rho GTPase that is regulated by Syd-1 and provide evidence that Rac1 promotes presynaptic development by promoting clustering of both Nrx-1 and Brp.

MATERIALS AND METHODS

DNA Constructs

New *syd-1* transgenes were created using a *UAS-syd-1-1xFLAG* DNA construct previously shown to rescue loss of *syd-1* from R7 photoreceptor neurons (Holbrook *et al.* 2012). Two new *UAS* full-length *syd-1* transgenes were created: (1) *UAS-syd-1^{wt}-3xFLAG* in which two additional FLAG tags were added to facilitate detection in pull-down experiments; and (2) *UAS-syd-1RA-3xFLAG*, which is identical to *UAS-syd-1^{wt}-3xFLAG* but has a substitution at codon 979 (numbered according to the fly Syd-1 isoform C; GenBank accession: AAF57207.2) causing it to specify alanine instead of arginine (R979A). DNA encoding the region from Q643 to M1164 (again numbered according to the isoform C sequence), which includes the predicted RhoGAP domain but lacks the C2 domain, was subcloned from each of the two new constructs into the pGEX-4T1 vector in such a way as to be in-frame with the N-terminal glutathione S-transferase (GST) open reading frame and an added C-terminal HA epitope tag, resulting in two new GST transgenes: *GST-syd1^{wt} GAP* and *GST-syd-1RA GAP*.

Biochemistry

Wild-type and constitutively-active mutant GST-Rac1, Rac2, Mtl, RhoA, RhoL, and Cdc42 fusion constructs were obtained from the *Drosophila* Genomics Resource Center. GST-fusion proteins, including GST-Syd-1^{wt} GAP and GST-Syd-1RA GAP, were expressed, in and purified from, *Escherichia coli* by standard methods (Amersham Pharmacia Biotech; Garcia-Mata *et al.* 2006). Total protein concentrations were determined by the Bradford protein assay, and protein purity by Coomassie Blue

staining of SDS-polyacrylamide gels. Flies containing *actin* (*act*)-*Gal4* [from the Bloomington *Drosophila* Stock Center (BDSC)] were crossed to flies containing the *UAS-syd-1^{wt}-3xFLAG* or *UAS-syd-1RA-3xFLAG*transgene. Lysates from the heads of adult progeny of both sexes were prepared as described in Emery (2007) and incubated with GST alone or a constitutively-active mutant GST-Rho GTPase bound to glutathione-Sepharose 4B resin (Amersham Pharmacia Biotech). After 1 hr on ice, samples were washed and analyzed by western blots probed with anti-FLAG antibody. GTPase activity assays were performed with EnzChek Phosphate Assay Kit (E-6646; Life Technologies).

Genetics and fly husbandry

Flies were grown on standard food at 25°. *BG380-Gal4* (Budnik *et al.* 1996) was used to drive expression of *UAS-Rac1^{wt}* (Luo *et al.* 1994), *UAS-Rac1^{V12}* (Luo *et al.* 1994), *UAS-syd-1^{wt}-1xFLAG* (Holbrook *et al.* 2012), or *UAS-syd-1RA-3xFLAG* (see above) in motorneurons; wild-type animals contained *BG380-Gal4* alone, *syd-1* mutant animals were *syd-1^{w46}/syd-1^{CD}*transheterozygotes that contained *BG380-Gal4* alone (Holbrook *et al.* 2012), and *trio* mutant animals were *trio^{S6A}/trio^{S137203}* transheterozygotes (Ball *et al.* 2010). In all cases, we analyzed females only.

NMJ dissections and staining

Late third-instar larval NMJs were dissected in Schneider's insect medium (Sigma-Aldrich) and fixed with Bouin's solution (Sigma-Aldrich) for 15 min. All samples,

except those stained with anti-Nrx-1 (see below), were then stained by standard methods: washed 3× in PBS containing 0.3% Triton-X 100 (PBT), blocked for 30 min in 5% normal goat serum, incubated with primary antibodies at 4° overnight, washed 3× with PBT, incubated overnight with secondary antibodies at 4° overnight, washed 3× with PBT, and mounted in Vectashield (Vector Laboratories). We used the following antibodies: fluorescence-conjugated anti-HRP (1:250; Jackson Immuno Labs); mouse anti-Brp (nc82, 1:100; Developmental Studies Hybridoma Bank); rabbit anti-FLAG (1:250; Sigma-Aldrich); mouse anti-Dlg (4F3, 1:250; Developmental Studies Hybridoma Bank); guinea pig anti-Nrx-1 (1:500; Li *et al.* 2007); rabbit anti-GluRIIC (1:2500; Marrus *et al.* 2004); all secondary antibodies (goat IgG coupled to Alexa Fluor 488, Alexa Fluor 555, or AlexFluor 633; 1:500) were from Life Technologies.

Quantifying NMJ bouton number

Each bar graph with this quantification (Figure 2, G and H, Figure 3F, and Figure 4, E and F) contains the results of a single experiment in which all genotypes were grown, dissected, and stained in parallel. Confocal images were collected on a Leica SP2 microscope (with a 63× 1.4 NA oil immersion objective) and analyzed with ImageJ software (Schindelin *et al.* 2012; http://fiji.sc/) (*n* = animals). Within each experiment, the images were randomized, and quantifications were performed blind to genotype. As is standard in the field, for each animal we counted the number of boutons (identified based on shape, as visualized by anti-HRP and anti-Dlg staining) on muscle 4 or on muscles 6/7 on both sides of segment A3 (*e.g.* Ball *et al.* 2010). As

is also standard, we divided bouton number by muscle area (measured in ImageJ by tracing the muscle perimeter visualized by anti-Dlg) to compensate for potential variations in animal size (Schuster *et al.* 1996; Ball *et al.* 2010). Note that we found no significant difference in muscle size among the genotypes tested (Supplemental Material, Figure S1).

Quantifying Nrx-1 levels

Each bar graph with this quantification (Figure 3J, Figure 5E, and Figure 7A) contains the results of a single experiment in which all genotypes were grown and dissected in parallel. Dissected pelts were notched in a genotype-specific pattern, and then all pelts were stained and washed in a single tube.

Staining for Nrx-1 was conducted as previously described (Li *et al.* 2007) using 0.05% Triton-X 100 and the Vectastain ABC system (Vector Laboratories) followed by Tyramide Signal Amplification (TSA; Life Technologies); TSA-treated NMJs were then incubated with fluorescence-conjugated anti-HRP (1:250; Jackson Immuno Labs) for 30 min at room temperature followed by washes with PBS.

Confocal images were collected on a Leica SP2 microscope and analyzed with ImageJ software (Schindelin *et al.* 2012; http://fiji.sc/) (*n* = animals). For each bar graph, all samples were imaged on the same day using the same laser settings and exposure, the images were randomized, and quantifications were performed blind to genotype (*n* = animals). For each animal, Nrx-1 levels were quantified within boutons on muscle 4 in segment A3. To do so, we used the anti-HRP channel to trace 4–10 presynaptic boutons while remaining blind to the anti-Nrx-1 channel; we duplicated

this trace and moved it to a region within the sample that did not contain anti-HRP staining; we then measured the average fluorescence intensities in the anti-Nrx-1 channel within each of the traces and subtracted the measurement outside the boutons from the measurement within boutons to obtain a final fluorescence value.

Quantifying BRP puncta size

The bar graph with this quantification (Figure 6F) contains the results of two experiments: one with *syd-1* genotypes and the other with *trio* mutants; wild-type animals were analyzed in each experiment (hence the two separate measurements of wild-type shown). In each of the two experiments, all genotypes were grown and dissected in parallel. Dissected pelts were notched in a genotype-specific pattern, and then all pelts were stained and washed in a single tube. Images were collected using three-dimensional (3D) structured illumination microscopy (SIM) with three grid rotations and five phases on a Zeiss Elyra S.1 inverted microscope with a Plan-Apochromat 63×/1.4 oil immersion lens. All samples were imaged on the same day using the same laser settings and exposure. Raw images were then batch-processed under identical settings using Zen software (Carl Zeiss). The reconstructed images were then analyzed by taking the maximum z-projections, and puncta sizes were quantified automatically by the "analyze particle" feature in ImageJ (http://fiji.sc/) (*n* = hemisegments).

Data availability and statistical analysis

Fly strains and DNA constructs are available upon request. For each experiment, genotypes and sample sizes are described in the legend of the corresponding figure. Because some transgenes were on the X chromosome, we analyzed females only for the sake of consistency. As described above, all experiments were scored blind to genotype. For each experiment a one-way ANOVA was conducted to determine if there was significant variation among genotypes. For experiments that showed a significant difference, individual *post hoc* pairwise comparisons were conducted between genotypes of interest by using either one- or two-tailed *t*-tests (see individual figure legends). For all figures: ns, not significant, * $P < 0.05$, ** $P < 0.01$, and *** $P < 0.001$. Exact *P* values are provided within the figure legends. Statistical values are presented as mean value ± SEM.

RESULTS

Drosophila Syd-1 Interacts With All Six Rho GTPases, and its Predicted GAP Domain Enhances the GTPase Activities of Rac1 and CDC42

Because the sequence of the RhoGAP-like domain fly Syd-1 suggested that it might be inactive (Hallam *et al.* 2002; Wentzel *et al.* 2013), we originally hypothesized that fly Syd-1 might simply bind Rho family GTPases without increasing their GTPase activity. To test this, we used GST pull-down assays to assess the abilities of each of the six fly Rho GTPases—three Racs, two Rhos, and one Cdc42—to interact with fly Syd-1. RhoGAPs preferentially bind the GTP-bound form of Rho GTPases, a form that can be transitory. To maximize the chance of observing this binding, we therefore used a mutant form of each fly Rho GTPase that stably mimics the GTP-bound form

(Garcia-Mata *et al.* 2006). We expressed and purified each of the six mutant fly Rho:GST fusions from *E. coli* and tested the ability of each one to pull down full-length FLAG-tagged fly Syd-1 from extracts of adult fly heads expressing FLAG-Syd-1 under the control of the ubiquitous *actin-Gal4* driver. We found that each of the six fly Rho GTPases is able to pull down the tagged fly Syd-1 in this assay (Figure 1A), consistent with our hypothesis that fly Syd-1 can bind Rho GTPases.

We next assayed whether fly Syd-1 has RhoGAP activity. Because full-length fly Syd-1 could not be expressed in *E. coli* cells, we GST-tagged and expressed a smaller fragment that included the RhoGAP but not the PDZ or C2 domains ("GST-Syd-1^{wt} GAP"). We purified this Syd-1 fragment and assayed its ability to increase the GTPase activities of each of the three major Rho family members in fly: Rac1, RhoA, and Cdc42. We found that the RhoGAP domain of fly Syd-1 significantly increases the GTPase activity of Rac1 and Cdc42 but not that of RhoA (Figure 1, B–D). The degree of increase is similar to that caused by the positive control p50 RhoGAP, which has previously been shown to increase the GTPase activity of all three Rho family members (Zhang *et al.* 1998). We conclude that, despite its noncanonical amino acid sequence, the RhoGAP-like domain of fly Syd-1 does have significant RhoGAP activity toward Rac1 and Cdc42.

Decreasing syd-1 Dosage Impairs the Ability of Wild-type but Not Constituitively-active Rac1 to Increase NMJ Bouton Number

We next wanted to test whether the GAP activity of fly Syd-1 might be required to regulate Rac or Cdc42 *in vivo*. Like Syd-1, both Rac1 and Cdc42 have previously been shown to act within motorneurons to regulate synaptic bouton number at fly NMJ (Rodal *et al.* 2008; Ball *et al.* 2010; Nahm *et al.* 2010). However, Cdc42 does so by attenuating retrograde BMP signaling, which is not known to be affected by Syd-1 loss. We therefore focused instead on testing whether Syd-1 might regulate Rac1. To do so, we took advantage of a genetic interaction test that was previously used to implicate the RacGEF Trio as a regulator of Rac1 at NMJ (Ball *et al.* 2010). Overexpression of Rac1 in motorneurons of wild-type animals significantly increases NMJ bouton number (Ball *et al.* 2010). While loss of one copy of *trio* has no effect on NMJ development in otherwise wild-type animals, it significantly impairs the ability of overexpressed Rac1 to increase bouton number (Ball *et al.* 2010). By contrast, $Rac1^{V12}$, which stably mimics the GTP-bound state of Rac1 (Luo *et al.* 1994), increases NMJ bouton number unimpaired by loss of *trio*. Together, these results suggest that Trio is required to potentiate Rac1, and does so by regulating the nucleotide-bound state of Rac1.

We used the same genetic interaction test to ask whether Syd-1 might also regulate Rac1. We found that overexpression of wild-type Rac1 or the mutant $Rac1^{V12}$ in motorneurons of wild-type animals significantly increases NMJ bouton number, as previously reported (Figure 2, A, D, G, and H). Loss of one copy of *syd-1* from otherwise wild-type animals has no effect on NMJ development in otherwise wild-type animals (Figure 2, A, B, G, and H). However, loss of one copy of *syd-1* does

prevent wild-type Rac1 from increasing NMJ bouton number (Figure 2, D, E, G, and H), indicating that, like Trio, Syd-1 is required to potentiate the ability of Rac1 to promote NMJ growth. Furthermore, loss of one copy of *syd-1* does not affect the ability of $Rac1^{V12}$ to increase NMJ bouton number (Figure 2, G and H), indicating that, like Trio, Syd-1 is only required to potentiate Rac1 that can change its nucleotide-bound state. We note that $Rac1^{wt}$ and $Rac1^{V12}$ increase synaptic bouton number to similar degrees at muscle 6/7 ($P = 0.38$), suggesting that the differential effect of *syd-1* dosage on the two proteins is unlikely to be caused by a difference in the strengths of their effects. [There may be a slight difference in the strengths of their effects at muscle 4, although it is not statistically significant in the data we have ($P = 0.057$).] These results are consistent with a model in which the GAP activity of Syd-1 directly regulates Rac1 by altering its nucleotide-bound state, but they do not rule out the possibility that the effect of Syd-1 on Rac1 is indirect.

We did note one difference between the effects of *trio* and *syd-1* loss on Rac1. Completely eliminating *trio* has no effect on the ability of $Rac1^{V12}$ to increase NMJ bouton number, indicating that the only role for Trio in this process is to promote the GTP-bound state of Rac1 (Ball *et al.* 2010). By contrast, we found that both $Rac1^{wt}$ and $Rac1^{V12}$ are significantly less able to increase NMJ bouton number in the complete absence of *syd-1* (Figure 2, A, F, G, and H). Since the GAP activity of Syd-1 would not be predicted to affect $Rac1^{V12}$, this result suggested that Syd-1 might have GAP-independent roles in promoting Rac1-induced NMJ growth, in addition to any GAP-dependent role it might have. We note that $Rac1^{V12}$ can increase bouton

number somewhat even in the absence of *syd-1* ($P = 2.8 \times 10^{-4}$ at muscle 4; but $P = 0.12$ at muscles 6/7), indicating that $Rac1^{V12}$ can act partly independently of Syd-1. To tease apart Syd-1's potential GAP-dependent and independent functions, we decided to create a mutant version of Syd-1 that specifically lacks GAP activity.

Overexpression of Wild-type or R979A Mutant Syd-1 in Wild-type Motorneurons Causes Similar Increases in NMJ Bouton Number and Nrx-1 Levels

Canonical RhoGAP proteins contain a conserved arginine that is required for their GAP activity (Scheffzek and Ahmadian 2005; Tcherkezian and Lamarche-Vane 2007). To test whether the same might be true of Syd-1, we constructed a GST-tagged Syd-1 RhoGAP domain in which we replaced the codon encoding this conserved arginine (at position 979, see *Materials and Methods*) with a codon encoding alanine (R979A; "GST-Syd-1^{RA}GAP"). We found that, indeed, the R979A substitution severely decreases the RhoGAP activity of Syd-1's RhoGAP domain (Figure 1, B–D). We next used the transgene encoding full-length wild-type Syd-1 (*UAS-syd-1^{wt}*; Holbrook *et al.* 2012) to create an equivalent transgene encoding R979A mutant Syd-1 (*UAS-syd-1^{RA}*). We tested whether, like other RhoGAP proteins with this R to A substitution, Syd-1^{RA} retains the ability to interact with Rho GTPases despite losing its GAP activity (Graham *et al.* 1999; Scheffzek and Ahmadian 2005). Indeed, we found that FLAG-tagged R979A mutant Syd-1 is pulled down from adult fly extracts by GST-tagged constitutively-active forms of all three major Rho family members: Rac1, RhoA, and Cdc42 (Figure 1E). We conclude that the R979A

substitution specifically disrupts Syd-1's GAP activity, providing us with a tool to analyze the latter's importance for Syd-1 function.

As a first test of the abilities of Syd-1^{wt} and Syd-1RA to promote synapse development, we overexpressed each in motorneurons of wild-type animals. We observed that, like endogenous Syd-1 (Owald *et al.* 2010), both Syd-1^{wt} and Syd-1RA localize to presynaptic puncta that are adjacent to and partly overlapping with the AZ protein Brp (Figure 3, A–B'), indicating that Syd-1's GAP activity is not required for its gross subcellular localization. Presynaptic Syd-1 is necessary and sufficient to recruit Nrx-1 to AZs (Owald *et al.* 2012), and overexpression of Nrx-1 is sufficient to increase NMJ bouton number (Li *et al.* 2007). We therefore predicted that presynaptic Syd-1^{wt} overexpression would increase both Nrx-1 levels and NMJ bouton number. Indeed, we found that overexpression of either Syd-1^{wt} or Syd-1RA significantly increases the number of boutons in wild-type animals; the effects of the two proteins are not significantly different (Figure 3, C–F). Using anti-Nrx-1 antibodies to quantify endogenous Nrx-1 levels, we found that overexpression of either Syd-1^{wt} or Syd-1RA also significantly increases Nrx-1 levels within NMJ boutons to similar degrees (Figure 3, G–J). We conclude that Syd-1's RhoGAP activity is not required for its ability to increase bouton number and promote Nrx-1 localization in wild-type animals.

Unlike Wild-type Syd-1, R979A Mutant Syd-1 Does Not Rescue the Decrease in NMJ Bouton Number in *syd-1* Mutants, Despite Restoring Nrx-1 Levels

Loss of *syd-1* causes a decrease in NMJ bouton number and a loss of Nrx-1 staining. We next wanted to compare the abilities of Syd-1^{wt} and Syd-1RA to rescue these defects in *syd-1* mutant animals. We expressed the two proteins in motorneurons of *syd-1^{w46}/syd-1^{CD}* transheterozyotes and found that Syd-1^{wt} fully rescues the decrease in NMJ bouton number (Figure 4, A–C, E, and F) but that Syd-1RA has no effect (Figure 4, A–F). We conclude that Syd-1RA's ability to increase NMJ bouton number in wild-type animals requires the presence of endogenous wild-type Syd-1 and that Syd-1's RhoGAP activity is required for normal NMJ growth. We confirmed that, as in wild-type animals, both Syd-1^{wt} and Syd-1RA form Brp-associated puncta in *syd-1* mutant animals (compare Figure 4, G and G' with Figure 3, A-B'), indicating that Syd-1RA's inability to rescue *syd-1*loss is not caused by a defect in its gross subcellular localization. This is the first evidence in any organism that Syd-1's GAP activity is required for presynaptic development.

We next wanted to pinpoint which of Syd-1's molecular functions depends upon its GAP activity. *syd-1* loss significantly decreases presynaptic Nrx-1 levels (Owald *et al.* 2012), and loss of *nrx-1* reduces NMJ bouton number to the same degree as loss of *syd-1* (Li *et al.* 2007; Owald *et al.* 2012). We therefore first tested whether the inability of Syd-1RA to rescue NMJ bouton number might be caused by an inability to recruit Nrx-1 in the absence of endogenous wild-type Syd-1. We again expressed Syd-1^{wt} or Syd-1RA in motorneurons of *syd-1* mutants and quantified anti-Nrx-1 staining within NMJ boutons. We found that, like Syd-1^{wt}, Syd-1RA is sufficient to

fully restore Nrx-1 to wild-type levels in *syd-1* mutant boutons (Figure 5). We conclude that Syd-1's RhoGAP activity is not required for its ability to localize Nrx-1.

Syd-1's RhoGAP Activity Is Required For Normal Brp Clustering, As Is the RacGEF Trio

In addition to binding and localizing Nrx-1, Syd-1 also directly binds and clusters Brp, a major structural component of AZs that is required for normal NMJ size (Kittel *et al.*2006; Owald *et al.* 2010). Loss of Syd-1 results in disorganized Brp puncta that are enlarged and irregularly spaced (Owald *et al.* 2010). We therefore next compared the abilities of Syd-1^{wt} and Syd-1RA to promote Brp clustering. We found that expressing Syd-1^{wt} in motorneurons fully restores the size of Brp puncta in *syd-1* mutants (Figure 6, A–C' and F), whereas expressing Syd-1RA has no effect on the Brp defect (Figure 6, D, D', and F). We conclude that Syd-1's RhoGAP activity is required for normal Brp clustering.

The obvious implication of this result is that Syd-1 regulates Brp, at least in part, by regulating the GTPase activity of one or more Rho proteins. Having already found biochemical and genetic evidence that Syd-1 regulates Rac1, we wanted to test whether Brp localization is disrupted by Rac1 loss. However, Rac1 is partly redundant with the other two fly *Rac* genes, and triple *Rac* mutant flies die early (Hakeda-Suzuki *et al.* 2002). We therefore chose instead to analyze Brp localization in animals lacking the Rac1 GEF Trio. Rac1 has been shown to be unable to promote NMJ bouton development in *trio*^{S6A}/*trio*^{S137203} null mutants, which nonetheless

survive until the end of larval development (Ball *et al.* 2010). We analyzed Brp puncta within the NMJ boutons of $trio^{S6A}/trio^{S137203}$ mutants and found them to be abnormally enlarged, like Brp puncta in *syd-1* mutants (Figure 6, E and F). We conclude that Trio, like Syd-1, is required for proper Brp clustering, consistent with a model in which their coregulation of Rac1 and/or other Rho GTPases is required for this process.

Syd-1 Is Required for Rac^{V12} to Increase Nrx-1 Levels

Finally, we wanted to follow up on our finding that complete loss of *syd-1* prevents $Rac1^{V12}$ from increasing NMJ bouton number. This result suggested that Syd-1 has one or more activities that are required for Rac1-induced NMJ growth but separate from Syd-1's effect on the nucleotide-bound state of Rac1. An obvious candidate for such an activity is Syd-1's recruitment of Nrx-1, since this occurs independently of Syd-1 GAP activity. If so, we would expect that: (1) $Rac1^{V12}$ overexpression promotes NMJ growth, at least in part, by increasing Nrx-1 levels; and (2) eliminating Syd-1 prevents $Rac1^{V12}$from causing this Nrx-1 increase. We tested these two predictions and, indeed, found that expressing $Rac1^{V12}$ in the motorneurons of wild-type animals causes a significant increase in Nrx-1 levels at NMJ (Figure 7A) and that complete loss of Syd-1 prevents this increase (Figure 7A). We conclude that Syd-1 participates with Rac1 in two separate functions that promote NMJ bouton development: (1) together with Trio, the RacGAP activity of Syd-1 is required to regulate the nucleotide-bound state of Rac1, which is required for normal Brp clustering; and (2) Syd-1, independent of its RacGAP activity, is

required for the recruitment of Nrx-1 to boutons, including the recruitment of Nrx-1 that is promoted by Rac1 (Figure 7B).

DISCUSSION

The Role of Syd-1's GAP Activity in Clustering Brp

In this paper, we have shown that Syd-1^{wt} and Syd-1^{RA} promote NMJ growth to similar degrees in wild-type animals and recruit similar levels of Nrx-1 to presynaptic boutons in both wild-type and *syd-1* mutants. However, unlike Syd-1^{wt}, Syd-1^{RA} is unable to restore Brp clustering in *syd-1* mutants, indicating that Syd-1's GAP activity is required for this process. Our results further suggest that Syd-1's GAP activity promotes Brp clustering by working together with the RacGEF Trio to potentiate Rac1. However, while loss of a GEF for Rac1 would be predicted to increase the proportion of GDP-bound, and therefore inactive, Rac1, we note that loss of a GAP for Rac1 should instead increase the proportion of GTP-bound, and therefore active, Rac1 (Scheffzek and Ahmadian 2005; Tcherkezian and Lamarche-Vane 2007). Why, instead, might loss of Syd-1 GAP activity impair Rac1 function at NMJ?

Given our finding that Syd-1's GAP domain also increases the GTPase activity of Cdc42, we considered the possibility that Syd-1 might potentiate Rac1 only indirectly, by acting upon Cdc42. The phenotype caused by Cdc42 loss from motorneurons—an increase in NMJ bouton number—is the same as that caused by Rac1 gain, suggesting that Cdc42 and Rac1 might antagonize one another during

NMJ development. Syd-1 loss might then impair Rac1 by increasing the proportion of GTP-bound, active Cdc42. However, we do not think this model is likely for three reasons. First, presynaptic loss of *cdc42*significantly enhances the formation of abnormally positioned "satellite" boutons, a hallmark of increased BMP signaling (Nahm *et al.* 2010), and we do not observe an increase in satellite boutons in animals overexpressing Syd-1^{wt} (or in *syd-1* mutants; Figure S2), suggesting that Syd-1 does not normally regulate Cdc42 at NMJ. Second, we directly tested whether coexpressing Cdc42 with Rac1 would impair the latter's ability to increase NMJ bouton number and found that it does not (Figure S2). Third, a model in which decreasing *syd-1* dosage potentiates a Rho GTPase with antagonistic effects on Rac1 does not explain the specific sensitivity of Rac1^{wt} and not Rac1^{V12} to this manipulation. Finally, we note that Syd-1 could also theoretically potentiate Rac1 indirectly by acting upon one of the other two fly Racs, if either of the latter were antagonistic to Rac1. However, there is no evidence of such antagonism: reducing the levels of one, two, or all three fly Racs has previously been shown either to have no effect or to decrease NMJ bouton number (Ball *et al.* 2010), and our third point (above) applies to this model too.

Our data are therefore more consistent with Syd-1 directly regulating the nucleotide-bound state of Rac1. In previous cases in which loss of the RhoGAP or RhoGEF for a single Rho GTPase causes the same defect, the explanation has been that the ability of the GTPase to cycle between GDP- and GTP-bound states is critical (Symons and Settleman 2000; Parrini and Camonis 2011; Sharif and Maddox

2012; Fritz and Pertz 2016); loss of the regulatory RhoGAP or RhoGEF then causes the same defect because either manipulation reduces the rate of Rho cycling. While it is theoretically possible that, instead, both GDP-bound and GTP-bound forms of Rac1 are separately required to promote Brp clustering at NMJ, there is no precedent for such a model: GDP-bound Rac1 is thought to be inactive (Symons and Settleman 2000; Parrini and Camonis 2011; Sharif and Maddox 2012; Fritz and Pertz 2016). We therefore favor a model in which Rac1 cycling is important for Brp clustering at NMJ.

How might Rac1 cycling affect Brp recruitment? Brp has previously been shown to directly bind *in vitro* to N- and C-terminal fragments of Syd-1 that lack the RhoGAP domain (Owald *et al.* 2010). One possibility is that the ability of Syd-1 to bind Brp *in vivo*is somehow regulated intramolecularly by the process of transforming a GTP-bound Rho GTPase into a GDP-bound form (simply binding the GTP-bound form would not be sufficient, since R979A Syd-1 binds all six Rhos yet cannot cluster Brp). Alternatively, Syd-1's RhoGAP activity may have an indirect effect on Brp by, in parallel, promoting a Rho GTPase-dependent change in presynaptic structure that facilitates the ability of Syd-1 to cluster Brp properly. Rho GTPases are classically involved in regulating actin assembly (Stankiewicz and Linseman 2014), and presynaptic development is characterized by the early appearance of actin-rich structures to which other molecules, including Syd-1, are recruited (Chia *et al.* 2012, 2013; Nelson *et al.* 2013). Perhaps Rac1, regulated by Syd-1 and Trio,

sculpts the local actin environment at presynaptic sites, creating a permissive environment for Syd-1 to recruit additional presynaptic components, including Brp.

The Roles of Rac1 and Syd-1 in Recruiting Nrx-1

In contrast to our evidence that Rac1 cycling may be important for Brp clustering, we found that $Rac1^{V12}$, which stably mimics the GTP-bound state, increases Nrx-1 levels in wild-type, and that Syd-1 lacking GAP activity is sufficient to increase Nrx-1 levels, even in the absence of endogenous Syd-1. These results suggest that Rac1 does not need to enter the GDP-bound state in order to promote Nrx-1 recruitment and that Rac1 cycling is therefore not required for this process. Nonetheless, complete loss of *syd-1* prevents Nrx-1 recruitment, even by $Rac1^{V12}$. Together, these results indicate that Syd-1 is required downstream of or in parallel to GTP-bound Rac1 to recruit Nrx-1 to boutons. Syd-1 and Nrx-1 have previously been shown to bind via an interaction between the former's PDZ domain and the latter's PDZ-binding domain; each protein depends on the other for its localization (Owald *et al.* 2012). One possibility is that Syd-1 localization or its ability to recruit Nrx-1 is potentiated by direct binding between Syd-1 and GTP-bound Rac1, an interaction of which $Syd\text{-}1^{RA}$ remains capable.

Fly Syd-1 Compared with Worm Syd-1 and Mouse mSYD1A

We have shown that fly Syd-1 requires its GAP activity to cluster the ELKS protein Brp. However, worm Syd-1 apparently lacks GAP activity and yet is able to cluster ELKS (Xu *et al.* 2015). How might this work? Both worm and fly Syd-1 also recruit

the scaffolding protein Liprin-alpha (Syd-2 in worm), which binds ELKS. Perhaps in worm this parallel mechanism of ELKS recruitment is sufficient for normal ELKS localization, alleviating the need for Rac cycling. Alternatively, some other RacGAP in worm might promote Rac cycling during synaptogenesis, creating a permissive environment for the GAP-dead worm Syd-1 to recruit ELKS.

By contrast, mouse mSYD1A does have GAP activity toward RhoA, but this activity is not required for its ability to rescue the presynaptic defects caused by mSYD1A loss (in cell culture at least; Wentzel *et al.* 2013). An obvious possibility is that the molecular mechanisms that promote presynaptic assembly differ substantially between vertebrates and invertebrates. However, we note that mice have a second Syd-1 homolog, mSYD1B, which has not yet been analyzed but which may have assumed some of the functions that depend on the single Syd-1 in invertebrates (Wentzel *et al.*2013). Consistent with this possibility, the presynaptic defects caused by mSYD1A loss are far milder than those of the invertebrate *syd-1* mutants (Wentzel *et al.* 2013). Because fly Syd-1RA can promote increased synaptogenesis in the presence of wild-type endogenous Syd-1, one possibility is that mouse mSYD1A lacking the RhoGAP domain can promote SV clustering in *mSYD1A^{KO}* knockout cells because wild-type mSYD1B is present. It will be interesting to examine the effects of deleting both mouse Syd-1 proteins and to test the functionality of mutant versions of those proteins in the double mutant animals. Fly Syd-1 was previously thought to lack RhoGAP activity in part because mouse mSYD1A GAP activity toward RhoA is eliminated by changing a single one of its residues into the corresponding fly

residue (Wentzel *et al.* 2013). Our results confirm that fly Syd-1's RhoGAP domain does not have GAP activity toward RhoA, but instead we found that it can regulate Rac1 and Cdc42. It will be interesting to see whether the GAP domain of mouse mSYD1B might share fly Syd-1's specificity.

BRIDGE TO CHAPTER III

My work in Chapter II demonstrates that Syd-1's GAP activity is required in-vivo for proper active zone clustering and synapse development. We also identified an interaction with the GTPase Rac1, which together with Syd-1, promotes NMJ development. Following initial synapse formation, these connections must be maintained throughout the life of the neuron. In Chapter III, I will detail a novel gene that our lab identified and describe its mechanism for maintaining and promoting synapse development through retrograde axonal transported of synaptic cargo.

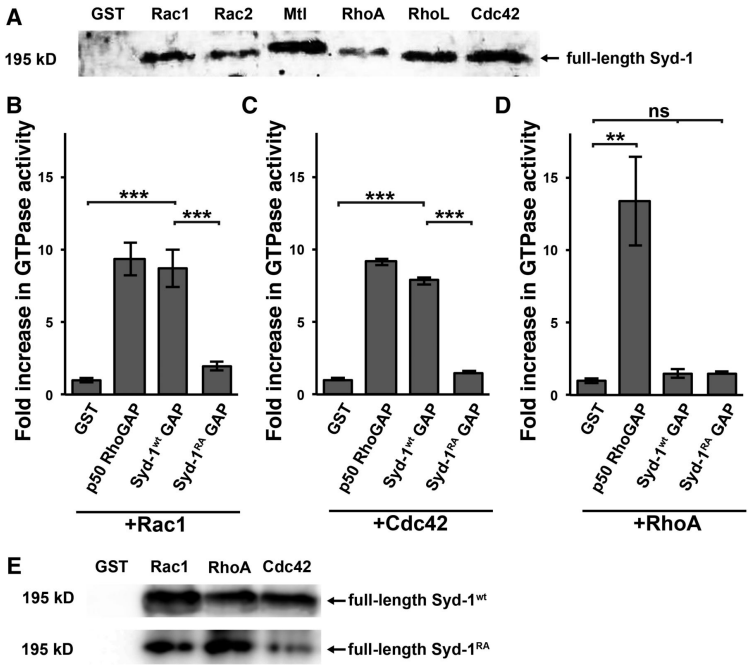

Figure 1. *Drosophila* Syd-1 interacts with all six Rho GTPases. Its predicted GAP domain enhances the GTPase activities of Rac1 and Cdc42 but not RhoA. (A) Western blot (probed with anti-FLAG antibodies) of protein pulled down by purified GST-Rho proteins. FLAG-tagged full-length wild-type fly Syd-1 expressed ubiquitously in adult head is pulled down by GST-tagged constitutively-active mutant forms of fly Rac1, Rac2, Mtl, RhoA, RhoL, or Cdc42, but not by GST alone. (B–D) Endpoint GTPase activity assays of wild-type fly Rac1 (B), Cdc42 (C), and RhoA (D). Each protein was assayed alone and in the presence of the negative control GST, the positive control p50 RhoGAP, the GAP domain of wild-type fly Syd-1 (Syd-1^{wt} GAP), or the GAP domain of fly Syd-1 in which the conserved arginine of the arginine finger is replaced by alanine (Syd-1^{RA} GAP). Activity is presented as fold-increase over the activity of each protein alone. Error bars represent SEM. *n*, Independent assays. As expected, GST does not increase the GTPase activity of Rac1 (1.00 ± 0.16, $n = 7$), Cdc42 (1.00 ± 0.09, $n = 3$), or RhoA (1.00 ± 0.22, $n = 3$), whereas p50 RhoGAP significantly increases the GTPase activity of all three (Rac1: 9.36 ± 1.16, $n = 7$, $P = 5.9 \times 10^{-6}$; Cdc42: 9.12 ± 0.22, $n = 3$, $P = 2.2 \times 10^{-6}$; RhoA: 13.32 ± 3.04, $n = 3$, $P = 0.0077$). We found that the wild-type GAP domain of Syd-1 significantly increases the GTPase activity of Rac1 (8.69 ± 1.29, $n = 7$, $P = 3.5 \times 10^{-5}$) and Cdc42 (7.83 ± 0.27, $n = 3$, $P = 9.0 \times 10^{-6}$) but not RhoA (1.48 ± 0.30, $n = 3$, $P = 0.13$). By contrast, the Syd-1^{RA} mutant GAP domain has a severely reduced ability to increase the GTPase activity of Rac1 (1.98 ± 0.31, $n = 7$, $P = 1.4 \times 10^{4}$), and Cdc42 (1.41 ± 0.08, $n = 3$, $P = 1.1 \times 10^{-5}$) and has no effect on RhoA (1.43 ± 0.18, $n = 3$, $P = 0.10$). * $P < 0.05$, ** $P < 0.01$, *** $P < 0.001$, based on one-tailed *t*-tests. (E) Like wild-type fly Syd-1 (Syd-1^{wt}), FLAG-tagged full-length R979A mutant fly Syd-1 (Syd-1^{RA}) expressed ubiquitously in adult head is pulled down by GST-tagged constitutively active mutant forms of Rac1, RhoA, and Cdc42 but not by GST alone.

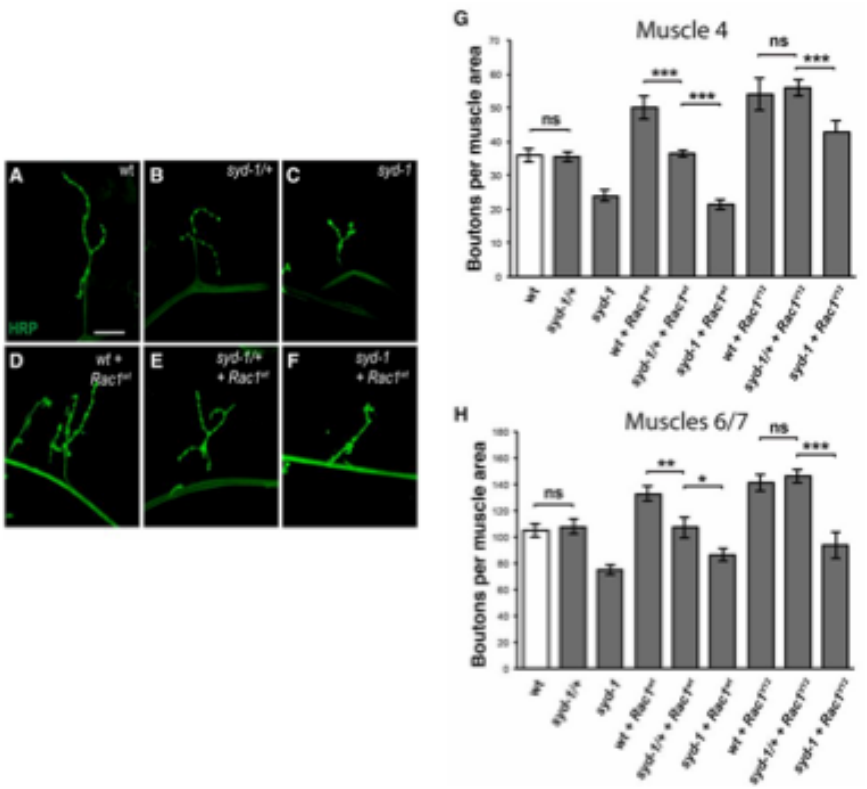

Figure 2. Wild-type Rac1, unlike Rac1^{V12}, requires wild-type Syd-1 levels in order to promote NMJ growth.

(A–F) Third-instar larval NMJs at muscle 4 in abdominal segment 3 stained with anti-HRP (green). Bar, 25 μm. All genotypes also contain the motorneuron driver *BG380-Gal4* and were costained with anti-Dlg. (A) Wild-type. (B) *syd-1^{CD}/+* heterozygote. (C) *syd-1^{CD}/syd-1^{w46}* mutant. (D) Wild-type animal in which motorneurons express wild-type Rac1 (Rac1^{wt}). (E) *syd-1^{CD}/+*heterozygote in which motorneurons express Rac1^{wt}. (F) *syd-1^{CD}/syd-1^{w46}* mutant in which motorneurons express Rac1^{wt}. (G) Quantification of the number of boutons on muscle 4 in abdominal segment 3 per muscle area. Loss of one copy of *syd-1* does not cause a decrease in bouton number (36.3 ± 1.3, *n* = 14) compared to wild-type (*BG380-Gal4* alone: 35.7 ± 1.9, *n* = 12). By contrast, while overexpressing wild-type Rac1 (49.5 ± 3.4, *n* = 12) significantly increases bouton number compared to the wild-type control (*P* = 0.0011), loss of one copy of *syd-1* prevents this increase (36.8 ± 1.0, *n* = 17, *P* = 1.9 × 10^{-8} compared to wild-type Rac1 in wild-type). By contrast, loss of one copy of *syd-1* has no effect on the increase in bouton number caused by overexpression of a constitutively-active form of Rac1, Rac1^{V12} (Rac1^{V12} alone: 58.5 ± 3.5, *n* = 8 (*P* = 4.8 × 10^{-5} compared to wild-type); Rac1^{V12} in *syd-1/+*: 56.0 ± 2.5, *n* = 12). Complete loss of *syd-1*impairs the ability of wild-type Rac1 (21.4 ± 1.6, *n* = 14, *P* = 1.9 × 10^{-8}) or Rac1^{V12} (36.6 ± 4.2, *n* = 11, *P* = 1.4 × 10^{-4}) to increase bouton number. Error bars represent SEM. *n* = animals. ns, not significant; *** *P* < 0.001, based on two-tailed *t*-tests. (H) Quantification of the number of boutons on muscles 6/7 in abdominal segment 3 per muscle area. We observed the same effects on bouton number as at both muscle 4. Wild-type (105.4 ± 3.1, *n* = 14) and *syd-1/+*heterozygotes

(108.0 ± 5.7, n = 14) have similar numbers of boutons. Overexpressing either wild-type Rac1 (133.0 ± 5.7, n = 14, $P = 1.3 \times 10^{-4}$) or $Rac1^{V12}$ (141.0 ± 6.5, n = 8, $P = 2.6 \times 10^{-5}$) causes an increase in bouton number. Removing one copy of *syd-1* prevents wild-type Rac1 from increasing bouton number (107.4 ± 8.1, n = 14, P = 0.0015 compared to wild-type Rac1 in wild-type) but has no effect on $Rac1^{V12}$ (146.0 ± 5.2, n = 17). Complete loss of *syd-1* impairs the ability of wild-type Rac1 (86.8 ± 5.0, n = 15, $P = 1.5 \times 10^{-6}$) or $Rac1^{V12}$ (93.5 ± 7.8, n = 14, $P = 5.3 \times 10^{-4}$) to increase bouton number. Error bars represent SEM. n = animals. ns, not significant; * $P < 0.05$, * $P < 0.01$, *** $P < 0.001$, based on two-tailed t-tests.

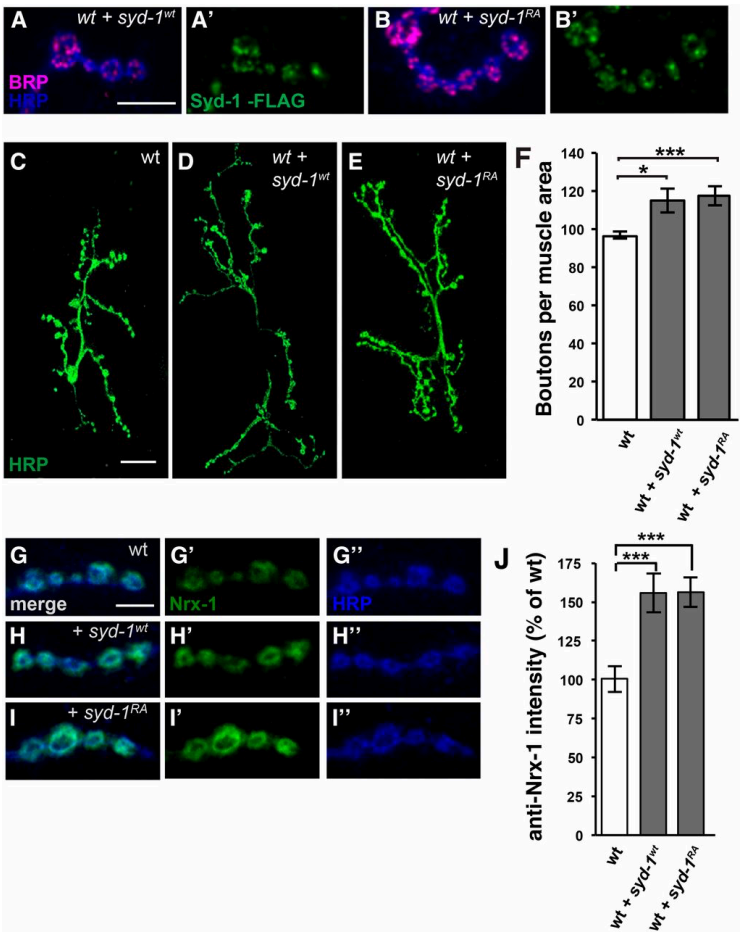

Figure 3. Wild-type and R979A mutant Syd-1 colocalize with Brp and cause similar increases in NMJ bouton number and Nrx-1 levels when expressed in wild-type motorneurons.

(A–B') Third-instar larval NMJ boutons on muscle 4 stained with anti-HRP (blue), anti-Brp (magenta), and anti-FLAG (green). Bar, 5 μm. (A and A') A wild-type animal in which motorneurons express wild-type full-length FLAG-tagged Syd-1 driven by *BG380-Gal4*. Like endogenous Syd-1, tagged wild-type Syd-1 forms puncta that are adjacent to, and partly overlapping with, the AZ protein Brp. (B and B') A wild-type animal in which motorneurons express R979A mutant full-length FLAG-tagged Syd-1 (Syd-1^{RA}) driven by *BG380-Gal4*. The punctate pattern and levels of Syd-1^{RA} resemble those of Syd-1^{wt}. (C–E) Third-instar larval NMJs at muscles 6/7 in abdominal segment 3 stained with anti-HRP (green). Bar, 25 μm. All genotypes also contain the motorneuron driver *BG380-Gal4*, and were costained with anti-Dlg. (C) Wild-type. (D) Wild-type in which motorneurons express wild-type full-length Syd-1. (E) Wild-type in which motorneurons express R979A mutant full-length Syd-1. (F) Quantification of the number of boutons on muscles 6/7 in abdominal segment 3 per muscle area. Overexpressing wild-type (114.9 ± 6.4, n = 10) or R979A mutant Syd-1 (117.8 ± 5.3, n = 7) causes similar, significant increases in bouton number (P = 0.02 and 5.9×10^{-4}, respectively) compared to the wild-type control (*BG380-Gal4* alone: 96.9 ± 1.8, n = 9). Error bars represent SEM. n = animals. * $P < 0.05$, *** $P < 0.001$, based on two-tailed t-tests. (G–I") Third-instar larval NMJ boutons on

muscle 4 stained with anti-HRP (blue) and anti-Nrx-1 (green). Bar, 5 μm. All genotypes also contain the motorneuron driver *BG380-Gal4*. (G–G″) Wild-type. (H–H″) Wild-type in which motorneurons express wild-type Syd-1. (I–I″) Wild-type in which motorneurons express R979A mutant Syd-1. (J) Quantification of anti-Nrx-1 staining. Overexpressing wild-type (155 ± 12.4%, $n = 14$) or R979A mutant Syd-1 (156 ± 9.4%, $n = 13$) significantly increases Nrx-1 levels in NMJ boutons ($P = p = 9.2 \times 10^{-4}$ and 3.1×10^{-4}, respectively) compared to the wild-type control (*BG380-Gal4* alone: 100 ± 8.4% $n = 15$). Error bars represent SEM. n = animals. ns, not significant; * $P < 0.05$, ** $P < 0.01$, based on one-tailed *t*-tests.

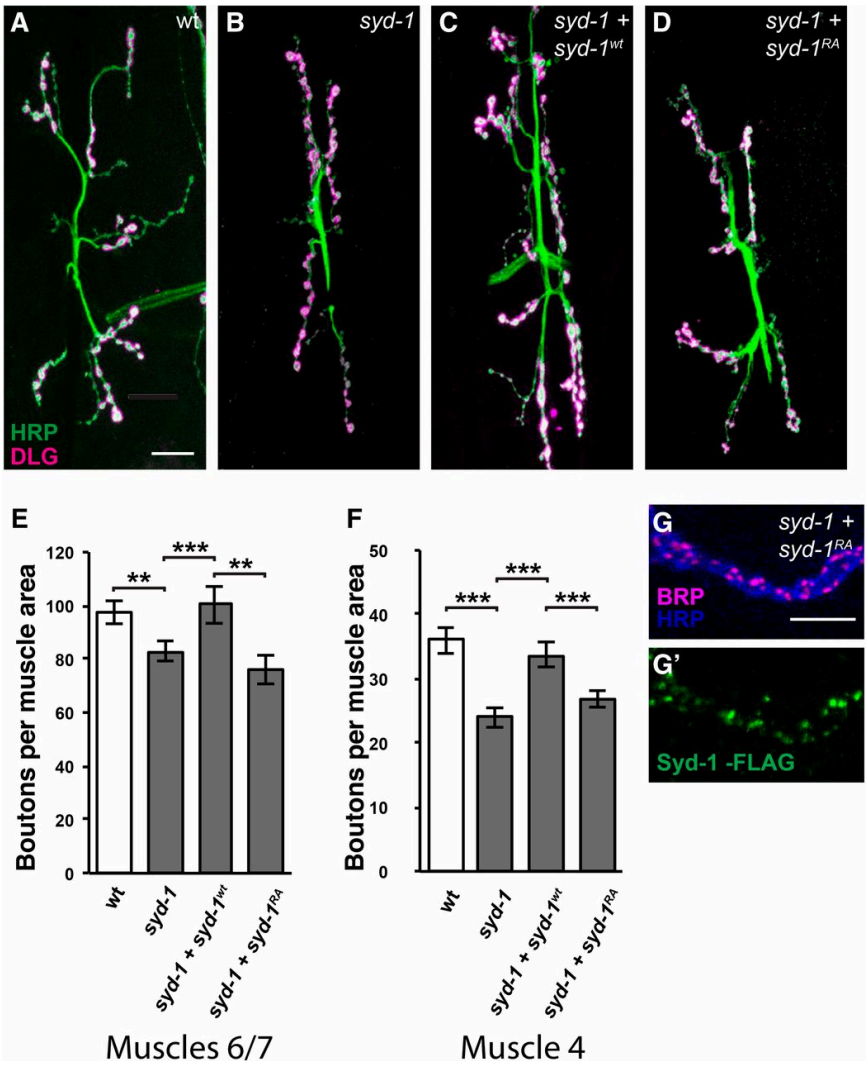

Figure 4. The decrease in NMJ bouton number in *syd-1* mutants is fully rescued by wild-type Syd-1 but unaltered by R979A mutant Syd-1.

(A–D) Third-instar larval NMJs at muscles 6/7 in abdominal segment 3 stained with anti-HRP (green) and anti-Dlg (magenta). Bar, 25 μm. All genotypes also contain the motorneuron driver *BG380-Gal4*. (A) Wild-type. (B) $syd\text{-}1^{CD}/syd\text{-}1^{w46}$mutant. (C) $syd\text{-}1^{CD}/syd\text{-}1^{w46}$ mutant in which motorneurons express wild-type Syd-1. (D) $syd\text{-}1^{CD}/syd\text{-}1^{w46}$ mutant in which motorneurons express R979A mutant Syd-1. (E) Quantification of the number of boutons on muscles 6/7 in abdominal segment 3 per muscle area. As previously reported, loss of *syd-1* causes a modest but significant decrease in NMJ bouton number (*BG380-Gal4* alone: 97.6 ± 4.5, $n = 14$; *syd-1* mutant: 82.6 ± 3.7, $n = 10$, $P = 3 \times 10^{-3}$). Overexpressing Syd-1^{wt} in the motorneurons of *syd-1* mutants rescues this defect (100.4 ± 7.0, $n = 10$, $P = 0.0018$). Overexpressing Syd-1^{RA} does not (76.0 ± 5.2, $n = 16$, $P = 0.0044$ compared to *syd-1* mutant expressing Syd-1^{wt}). Error bars represent SEM. n = animals. ns, not significant; * $P < 0.05$, ** $P < 0.01$, based on one-tailed *t*-tests. (F) Quantification of the number of boutons on muscle 4 in abdominal segment 3 per muscle area. Again, loss of *syd-1* decreases NMJ bouton

number (*BG380-Gal4* alone: 36.0 ± 2.1, n = 12; *syd-1* mutant: 24.0 ± 1.6, n = 10, $P = 5.5 \times 10^{-5}$), and presynaptically expressed Syd-1^{wt} rescues this defect (33.7 ± 1.9, n = 12, $P = 9.9 \times 10^{-5}$), but Syd-1^{RA} does not (26.8 ± 1.2, n = 13, $P = 7.9 \times 10^{-4}$compared to *syd-1* mutant expressing Syd-1^{wt}). Error bars represent SEM. n = animals. ns, not significant; *** $P < 0.001$, based on two-tailed t-tests. (G and G') Third-instar larval NMJ boutons on muscle 4 of *syd-*1^{CD}*/syd-*1^{w46} mutant animals in which motorneurons express R979A mutant full-length Syd-1 driven by *BG380-Gal4*, stained with anti-HRP (blue), anti-Brp (magenta), and anti-FLAG (green) as in Figure 3, A–B'. Bar, 5 μm. As in wild-type, tagged R979A mutant Syd-1 expressed in *syd-1* mutant motorneurons forms puncta that are adjacent to and partly overlapping with Brp. Note, however, that the endogenous Brp puncta appear somewhat abnormal (see Figure 6).

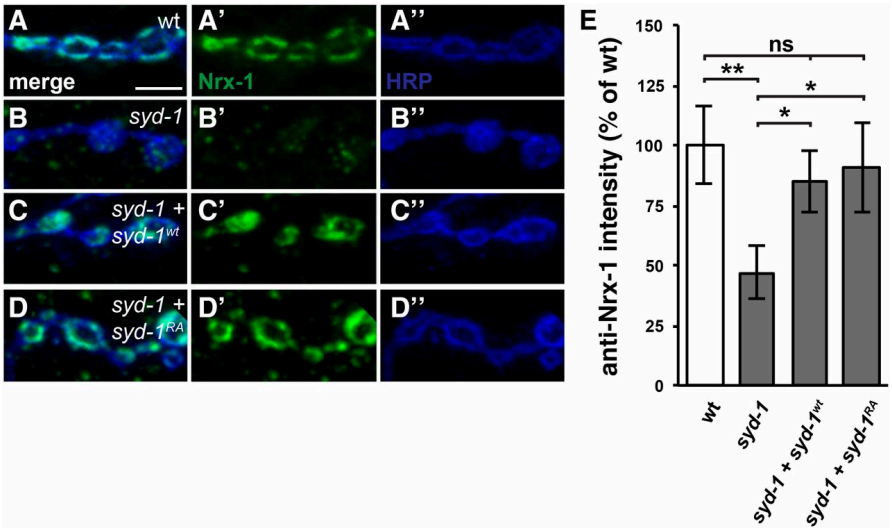

Figure 5 Both wild-type and R979A mutant Syd-1 fully restore NMJ Nrx-1 levels in *syd-1* mutants.

(A–D") Third-instar larval NMJ boutons on muscle 4 stained with anti-HRP (blue) and anti-Nrx-1 (green). Bar, 5 μm. All genotypes also contain the motorneuron driver *BG380-Gal4*. (A–A") Wild-type. (B–B") *syd-1^{CD}/syd-1^{w46}* mutant. (C–C") *syd-1^{CD}/syd-1^{w46}* mutant in which motorneurons express wild-type Syd-1. (D–D") *syd-1^{CD}/syd-1^{w46}* mutant in which motorneurons express R979A mutant Syd-1. (E) Quantification of anti-Nrx-1 staining. As previously reported, loss of *syd-1* decreases Nrx-1 levels in presynaptic boutons (*BG380-Gal4* alone: 100 ± 16%, n = 13; *syd-1* mutant: 47 ± 11%, n = 12, P = 0.0043). Overexpressing either wild-type or R979A mutant Syd-1 in the motorneurons of *syd-1* mutants rescues this defect (85 ± 13% (n = 12, P = 0.013) and 91 ± 19% (n = 9, P = 0.021), respectively). Error bars represent SEM. n = animals. ns, not significant; * $P < 0.05$, ** $P < 0.01$, based on one-tailed t-tests.

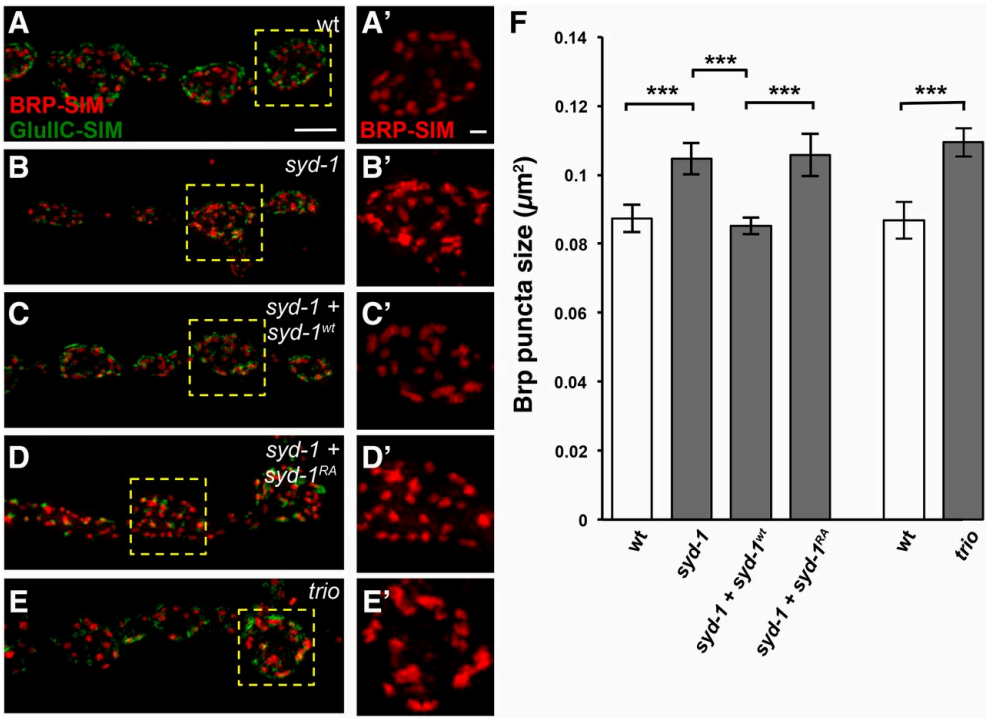

Figure 6. The defect in Brp clustering in *syd-1* mutants is fully rescued by wild-type Syd-1, unaltered by R979A mutant Syd-1, and phenocopied by loss of the RacGEF Trio.

(A–E') SIM images of third-instar larval NMJ boutons on muscle 4 stained with anti-Brp (red) and anti-GluRIIC (green). Bar, 1 μm. Genotypes in (A–D') also contain the motorneuron driver *BG380- Gal4*. (A and A') Wild-type. (B and B') *syd-1^{CD}/syd-1^{w46}* mutant. (C and C') *syd-1^{CD}/syd-1^{w46}* mutant in which motorneurons express wild-type Syd-1. (D and D') *syd-1^{CD}/syd-1^{w46}* mutant in which motorneurons express R979A mutant Syd-1. (E and E') *trio^{6A}/trio^{S137203}* mutant. (F) Quantification of the average size of anti-Brp puncta. As previously reported (Owald *et al.*2010), loss of *syd-1* increases the average size of anti-Brp puncta (0.105 ± 0.004 μm^2, n = 17) compared to wild-type (0.087 ± 0.004 μm^2, n = 21, $P = 3.0 \times 10^{-4}$). Overexpressing Syd-1^{wt} in the motorneurons of *syd-1* mutants rescues this defect (0.085 ± 0.002 μm^2, n = 14, $P = 6.3 \times 10^{-4}$). By contrast, overexpressing Syd-1RA in the motorneurons of *syd-1*mutants does not (0.106 ± 0.006 μm^2, n = 12, $P = 9.7 \times 10^{-4}$ compared to *syd-1* mutant expressing Syd-1^{wt}). In a separate experiment, we found that loss of Trio increases the average size of anti-Brp puncta (0.109 ± 0.004 μm^2, n = 14, $P = 1.2 \times 10^{-4}$) to a degree similar to that caused by loss of Syd-1. Error bars represent SEM. n = hemisegments. ns, not significant; ** $P < 0.01$, *** $P < 0.001$, based on one-tailed t-tests.

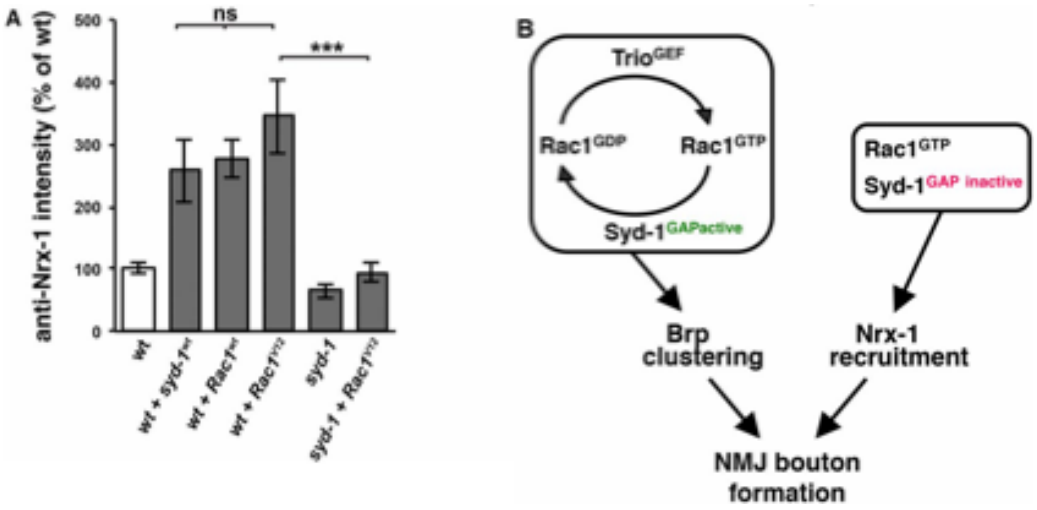

Figure 7. Rac1^{V12} requires Syd-1 in order to increase Nrx-1 levels at NMJ.
(A) Quantification of anti-Nrx-1 staining. Overexpressing either Rac1^{wt} or Rac1^{V12} in the motorneurons of wild-type animals increases Nrx-1 levels in presynaptic boutons [to 278 ± 31%, n = 14, $P = 4.3 \times 10^{-6}$, or 345 ± 60%, n = 16, $P = 4.7 \times 10^{-4}$, of wild-type levels, respectively (*BG380-Gal4* alone: 100 ± 9%, n = 15)]. Loss of *syd-1* significantly impairs the ablility of Rac1^{V12} to increase Nrx-1 levels (94 ± 16%, n = 8, $P = 1.2 \times 10^{-4}$ compared to Rac^{V12} in wild-type). Error bars represent SEM. n = animals. ns, not significant; * $P < 0.05$, ** $P < 0.01$, *** $P < 0.001$, based on one-tailed t-tests. (B) Model. Previous work has shown that Syd-1 is required presynaptically for the recruitment of Nrx-1 and clustering of Brp at NMJ, and that each of these processes is required for the formation of a wild-type number of NMJ boutons. In this paper, we provide evidence that Syd-1's GAP activity is required together with the RacGEF Trio to promote proper Brp puncta size by regulating the nucleotide-bound state of Rac1. The similarity between the Brp defects caused by *syd-1* or *trio* loss suggests that Rac1 cycling between GTP- and GDP-bound states is required for normal Brp clustering (see *Discussion*). By contrast, we find that Syd-1 does not require RacGAP activity to recruit Nrx-1 to boutons and that GTP-bound Rac1 is sufficient for this process but that Rac1 cannot increase Nrx-1 levels in the absence of Syd-1. See *Discussion* for more details.

CHAPTER III

IDENTIFYING AND CHARACTERIZING VEZATIN-LIKE, A NOVEL GENE REQUIRED FOR RETROGRADE AXONAL TRANSPORT

INTRODUCTION

Axonal transport plays a key role in the establishment and maintenance of synapses through the transport of synaptic components, relay of signaling pathways and removal of senescent components and debris that accumulate in aged neurons (Maday et al. 2014). This process is facilitated through the linking of cargo to two types of motor proteins: kinesins, which undergo anterograde movement towards the plus end of microtubules, and dynein, which moves retrogradely towards the cell body (Piling et al. 2006). The ability for neurons to utilize both motors proteins and establish bidirectional transport is essential for the proper distribution of synaptic components and the function and survival of the neuron (Wong et al. 2012).

Retrograde axonal transport is critical for the formation and maintenance of neural circuits through the delivery and recirculation of dense core vesicles containing neuropeptides, endosomes to maintain homeostasis within the neuron (Peterson et al. 2018). Retrograde axonal transport has become of particular interest as of late as neurons in several human diseases including Alzheimer's, ALS and Parkinson's

disease have shown to have defects in retrograde transport (Perlson et al. 2012). Despite this importance, it remains unknown how dynein is capable of binding a variety of cargo that have unique spatial and temporal regulation.

Emerging evidence in the field has identified a series of dynein adaptors; proteins that facilitate and regulate cargo-specific binding to dynein and regulate dynein processivity. Several of these adaptor and regulatory proteins have already been identified, including dynactin, a large multisubunit protein that forms a co-complex with dynein (Karki et al. 1995, Vaughan et al. 1995) and enhances the recruitment of dynein to microtubules (Chowdhury et al. 2015) as well as mediating binding to certain intracellular cargos (Holleran et al. 2011, Zhang et al. 2011). Another adaptor also identified is HookA, an adaptor of early endosomes to dynein, (Zhang et al. 2014, Guo et al. 2016). It's predicted that more cargo adaptors exist to provide for the variety of cargo (Olenick et al. 2016).

Recently, a distant and putative Vezatin homologue in *Aspergillus Nidulans* has been found to be required for the initiation of dynein-mediated retrograde transport of early endosomes in hyphal tips through binding to HookA (Yao et al. 2015). Vertebrate Vezatin is a large scaffolding protein that has variety of functions including binding to the FERM domain of myosin VIIa and maintaining tight junction formation (Kussel-Andermann et al. 2000), and promoting dendrite spine morphology by binding to the GTPase Arf6 (Sanda et al. 2010), but it has yet to be implicated in regulating axonal transport.

Here we identify and characterize a previously unstudied *Drosophila* gene, Vezatin-like, which shares homology with mammalian Vezatin and is required for proper retrograde transport in *Drosophila*. Vezatin-like was identified by the presence axon terminal swellings and axonal cargo accumulation resembling a mutation within the dynactin subunit $p150^{Glued}$ (Llyod et al. 2012). However, unlike most mutations in molecular motors which affect bi-directional transport, we find that the *vezl* mutation specifically accumulation cargo undergoing retrograde transport. We find that Vezl is localized along microtubule tracts and is enriched in distal tips. Using live imaging, we found that this defect is exacerbated in early endosomes and reveals that early endosomes have impaired retrograde transport and often fail to exit the distal tips of neurons.

MATERIALS AND METHODS

Generation of Vezatin-like fly stocks

CG7705 null flies were generated by imprecise P-element excision screen. Flies containing a P-element in the 5' coding region of CG7705 (FBal0244292, Flybase) were crossed flies carrying a transposase. Progeny that lost the w^+ minigene and failed to complement *721* for lethality; were sequenced to identify a deletion within CG7705. Expression constructs were generated from full length CG7705 cDNA from the Berkeley Drosophila Genome Project (LP22035, DGRC) and full-length human cDNA for Vezatin (Accession:BC064939, obtained from Dharmacon). Constructs were sequence verified then cloned into pUAST expression vectors containing either

a c-terminal Venus or N terminal 5xFLAG tag (Wang et. al, 2012, Addgene plasmid 35204 & 35201 respectively) using Gateway technology (Thermofisher). Constructs were then injected into wild-type larvae larvae containing attp8 site on the X-chromosome (BestGene) and screened for eye color and sequence verified.

Other fly stocks

Drosophila stocks used in this study are as follows:
UAS-ANF-EMD (#7001), UAS-Mito (#8442)UAS-Rab5 (#50788) UAS-Rab7 (#42705) UAS-Rab 11 (#8506) Mhc-Gal4 (#55132) Ok371-Gal4 (#26160) were all obtained from Bloomington Drosophila Stock Center. UAS-Tkv-mCherry was a generous gift from Dr. Kornberg (Roy et al. 2014)

NMJ dissection and staining

Late third-instar larval NMJs were dissected in Schneider's insect medium (Sigma-Aldrich) and fixed with Bouin's solution (Sigma-Aldrich) for 15 min and then stained by standard methods: washed 3× in PBS containing 0.3% Triton-X 100 (PBT), blocked for 30 min in 5% normal goat serum, incubated with primary antibodies at 4° overnight, washed 3× with PBT, incubated overnight with secondary antibodies at 4° overnight, washed 3× with PBT, and mounted in Vectashield (Vector Laboratories). We used the following antibodies: fluorescence-conjugated anti-HRP (1:250; Jackson Immuno Labs); mouse anti-Brp (nc82, 1:100; Developmental Studies Hybridoma Bank); rabbit anti-GFP (1:250; Sigma-Aldrich); mouse anti-Dlg (4F3, 1:250; Developmental Studies Hybridoma Bank); guinea pig anti-Nrx-1

(1:500; Li *et al.* 2007); rabbit anti-GluRIIC (1:2500; Marrus *et al.* 2004); all secondary antibodies (goat IgG coupled to Alexa Fluor 488, Alexa Fluor 555, or AlexFluor 633; 1:500) were from Life Technologies.

Live imaging and velocity measurements

Live imaging was done with either a Zeiss lm780 or Elyra SP2 microscope. Videos were recorded with a minimum of 2FPS over the course of 6-10min timespans. Live samples were prepared and dissected as previously describe (Spinner & Walla, 2018) in Ca^{2+}-free HL3.1 buffer. Section A3 of the larval NMJ was used for live imaging and bouton recording were carried out at muscle 4. All samples were carried in a controlled climate and conducted during similar times in the day. Velocities were measured from the slopes of kymographs generated by the multikymograph tool in Image J (Schindelin *et al.* 2012; http://fiji.sc/).

RESULTS

Vezatin-like (Vezl) is required for normal photoreceptor axon terminal morphology

From a forward genetic screen in *Drosophila* we identified a novel EMS induced loss-of-function mutation, *721*, that caused aberrant synaptic development in R7 photoreceptors (Figure 1). The *721* was found to be homozygous lethal, so we generated GMRFLP/MARCM clones that produced a percentage R7s homozygous for the mutation in an otherwise wild-type background. While wild-type R7s normally

tile the medulla and terminate at the M6 target layer in ellipsoid boutons (Figure 1B), R7's clones homozygous for the *721* mutation appeared to frequently have extensions past the target layer and terminated with a bulbous tip (Figure 1C). The causative mutation was mapped to an uncharacterized gene, previously annotated as Candidate Gene 7705 (CG7705, Figure 1A). Position-Specific Iterative (PSI)-BLAST showed that CG7705 most closely resembles the mammalian protein Vezatin, leading us to rename CG7705 to Vezatin-like (Vezl). The relation between CG7705/Vezl is further explored in the Discussion.

To verify that *vezl* loss was causative of the overextensions in R7s, we generated a targeted deletion of the *vezl* locus, $vezl^{13.1}$ as well as a UAS-*vezl* transgene (Figure 1A). We found that loss of *vezl* phenocopied the *721* mutation in R7s (Figure 1D) and expression of UAS-*vezl* in mutant R7's was able to fully rescue the defects in both the *721* mutant and *vezl* null backgrounds (Figure 1E). Therefore, we have identified a novel function for Vezl in synapse development.

Loss of Vezl results in defects in NMJ development and distal bouton morphology

To further address how Vezl may be affecting neural development and synapse formation, we moved from R7s to the larval neuromuscular junction (NMJ). The *Drosophila* NMJ has been a widely used model system in studying synapse development in part for its tractability and relative large synapse that are readily accessible for immunolabeling and visualization. In third-instar *vezl* mutant larvae,

we found that overall NMJ size was drastically reduced compared to control (Figure 2A and 2B). Pre-, but not postsynaptic expression of Vezl-cDNA was able to fully rescue this defect (Figure 2D), indicating that Vezl is necessary and sufficient for NMJ development and that Vezl's requirement in synapse development is not neuron-type specific.

We also noticed that *vezl* mutant larvae's distal boutons were enlarged in size compared to wild-type animals (Figure 2E-G). In addition, these distal boutons also abnormally accumulated the neuronal membrane marker α-HRP in the interior of the bouton and frequently had satellite boutons (Figure 2H and 2I). In fly NMJ, synapses are observed by the presence of presynaptic active zones that directly oppose postsynaptic glutamate receptors (Figure 2J). In *vezl* mutant larvae, regions that were positive for excessive α-HRP staining show an absence of both active zones and glutamate receptors and had and overall reduction in the density of synaptic sites (Figure 2K and 2L). As with R7's, these phenotypes were only observed in the distal most regions of the neuron while the rest of the boutons appeared unperturbed by Vezl loss. Altogether, this indicates a unique function at neuron tips that is shared between neuron types.

Vezl promotes NMJ growth, localizes to microtubules, and is enriched in distal boutons.

Since Vezl expression is required for normal NMJ size, we wanted to test if increasing expression of Vezl using the UAS-*vezl*-Venus transgene could further

promote NMJ growth. We found that overexpression caused a gain of function phenotype resulting in increased NMJ size as well as the formation of satellite boutons (Figure 3A-C). These satellite boutons were found throughout the length of the NMJ, as opposed to the satellite boutons in *vezl* mutants that were only found off of distal boutons (Figure 2B). We then tested Vezl localization in motor neurons with our Venus-tagged transgene. When expressed with a motor neuron specific Gal4, Vezl-Venus was observed along the length of the motor neuron where it was confined to the center of axon and was enriched in distal boutons where it had a more diffuse expression pattern further suggesting a function neuron tips (Figure 3E).

Vezl mutants have normal synaptic vesicle distribution, but excessive endosome accumulation

A general decrease in NMJ size is caused by disruptions in many different developmental pathways in *Drosophila*, and is not particularly insightful to characterization of Vezl's role in development. However, the swelling and accumulation of neuronal membrane at distal tips is far more rare. One of the few mutations that cause a similar phenotype is a mutation in the *Glued* locus encoding the dynactin subunit $p150^{Glued}$ (Llyod et al. 2012). This mutation resulted in the failure of dynein reattachment to microtubules and therefore a disruption of retrograde transport that caused an excessive accumulation of synaptic cargo in distal boutons (Llyod et al. 2012). Based on this and the similarity in morphology

with the dynactin mutant, we decided to test whether loss of Vezl similarly disrupts retrograde transport.

Using a combination of antibodies and fluorescently tagged transgenes, we tested which, if any, of the commonly trafficked proteins and molecules might accumulate abnormally in distal boutons. The mutation in $p150^{Glued}$ resulted in accumulation of synaptic vesicles and dense core vesicles in distal boutons (Llyod et al. 2012). In contrast to what was seen in dynactin mutants, synaptic vesicle markers synaptotagmin (syt) and cysteine string protein (CSP) were not enriched in distal boutons of *vezl* mutant larvae and appeared to have normal expression compared to wild-type (Figure 4A-D). However, we did find a slight increase in the amount of dense core vesicles that accumulated in distal boutons of *vezl* mutant animals compared to wild-type (Figure 4E-F, 4M).

Dense core vesicles undergo anterograde transport to delivery neuorpeptides to synapses, but recirculate throughout the life of the neuron to maintain protein homeostasis. We wondered whether other cargo that undergoes retrograde transport might similarly be enriched by looking at the expression of endosomes. Rabs are a large family of GTPases that bind to vesicles in a stereotyped manner and dictate intracellular compartment localization and they are exchanged with other Rab members as the vesicles transition in either transport or function (Bucci et al. 2014). Thus, Rabs are frequently used to identify different stages of vesicle transport: Rab5 for early forming endosomes, Rab7 for late endosomes undergoing

retrograde transport and Rab11 for recycling endosomes (Bucci et al. 2014). We used transgenes for Rab5, Rab7 and Rab11 and looked for their localization in *vezl* mutants. We found that endosomes positive for Rab5 and Rab7 were accumulating in distal boutons (Figure 4G-J and 5M), but not Rab11 (Figure 4K-M). Therefore loss of Vezl appears to have specificity towards cargo that undergoes retrograde transport.

Retrograde BMP signaling is affected by Vezl loss

BMP signaling is one of the major signaling pathways to promote activity-dependent NMJ growth during larval development (Bayat et al. 2011). The BMP pathway is initiated by a muscle-derived release of the Gbb ligand to its presynaptic co-receptors Wishful thinking (Wit), Saxophone (Sax) and Thick veins (Tkv) whom then phosphorylates MAD (pMAD) which translocates to the nucleus and activates pathways required for NMJ growth (Smith et al. 2012). This process is dependent on the ability of activated Wit, Sax and Tkv to be endocytosed and undergo retrograde transport back to the soma through Rab5 and Rab7 positive endosomes (Roy et al. 2014). Loss of BMP signaling results in reduced NMJ size (Ball et al. 201o), and elevated BMP signaling results in increased NMJ growth that is often accompanied by the formation of satellite boutons (Ball et al. 2010). Based on the similarity in dependence between BMP and Vezl expression levels and NMJ size, as well the BMP pathway's dependence on retrograde transport, we hypothesized that BMP signaling components may also be accumulating in distal boutons and failing to reach the nucleus in *vezl* mutants.

As with endosomes, antibody staining against pMAD had increased levels in distal boutons compared to the distal boutons in wild-type larvae (Figure 5A-B and 5E). To test if the accumulation of pMAD was the result of a failure co-receptors to be endocytosed and transported, we used a Tkv-mCherry transgene that is known to undergo retrograde transport to the soma in Rab7 positive vesicles (Roy et al. 2014). Expression of Tkv-mCherry in the motorneurons in of wild-type animals was normally localized throughout the NMJ as previously reported (Roy et al. 2014) (Figure 5C), however loss of *vezl* resulted in increased distal accumulation of the Tkc-mCherry transgene (Figure 5D-E) similar to that seen with Rab5 and Rab7.

Defects in axonal transport in motor neuron axons

To determine whether the accumulation of endosomes and BMP markers is due to a failure of transport or due to an increase in endocytosis, we used live imaging to analyze the movements of the axonal transport markers that we observed in fixed preparations. As previously mentioned, Anf-GFP positive vesicles normally circulate through the nervous system bidirectionally but accumulated in greater amount in distal tips of *vezl* mutants (Figure 4F). We first looked in motor neuron axons for gross defects in axonal transport by tracking vesicle dynamics in real time. In wild-type live-animals we observed that that majority of the labeled vesicles were actively moving and their directionality was evenly split between anterograde and retrograde (Figure 6A and 6C). In *vezl* mutant larvae, there were several noticeable transport defects including an overall decrease in the number dense core vesicles

that were visible and moving in the axon (Figure 6E), and those that were moving, were predominately undergoing anterograde transport and very few, if any, were undergoing retrograde transport (Figure 6C). Additionally, a large population of the labeled vesicles remained stationary during the course of imaging (Figure 6D). Anterograde and retrograde velocities of the moving vesicles were recorded but there was not a significant difference in either (Figure 6F).

We then looked to see whether transports of Tkv-mCherry labeled vesicles were similarly affected. We first noted that even though Tkv-mCherry labeled fewer vesicles than ANF-GFP, there were still noticeable defects in transport that appeared to specifically affect retrograde movement similar to what was seen with ANF-GFP including an increased number of stationary vesicles and fewer, if any, retrograde moving vesicles and reduced overall density in *vezl* mutants (Figure 7A-E). Further, save for a slight decrease in anterograde movement velocity in mutant larvae, there were no significant changes in the vesicles velocities (Figure 7F). Similar cargo stalls in axons have been attributed to mutations affecting the binding affinity of dynein to its cargo or to microtubules. While they are able to move with normal kinetics, they eventually release from the tracts and remain stalled within the axon (Smith and Gallo 2018). Based off of our observations and the similarities witnessed in these mutants, Vezl is most likely affecting the binding of the motor to its cargo rather than affecting the actual kinetics of motor.

We also tested whether these defects in transport were specific to retrograde moving endosomes by looking at the transport of mitochondria, which has a highly characterized transport profile (Smith et al. 2017). We did not notice any observable change in velocity, flux or percentage of stationary vesicle between wild-type and *vezl* mutant animals (Supplemental figure 1), indicating a cargo-specific role for Vezatin in axonal transport.

Defects in axonal transport at boutons

How are endosomes accumulating in distal boutons? Based on the observed defects in retrograde transport in axons, we hypothesized that the accumulation of synaptic cargo in distal boutons may be the result of a failure of endosomes to undergo retrograde transport. We again utilized ANF-GFP, now looking specifically at movement in and out of the distal boutons. Similar to fixed samples, live animals had boutons that were filled with ANF-GFP positive vesicles (Figure 8A). To accurately track the movement of individual vesicles we used fluorescence recovery after photobleaching (FRAP) to photobleach the second to last bouton and measure the number of vesicles that entered the bleached area either from the distal bouton (through retrograde transport) or the proximal bouton (through anterograde transport). In control animals we observed a roughly equal distribution of anterograde and retrograde moving vesicles (Figure 8A), and even in *vezl* mutant animals the vesicle flux appeared unperturbed (Figure 8B and 8C).

However, when we did comparable experiment with Tkv-mCherry we noticed a significant difference. In live wild-type animals, Tkv labeled vesicles underwent both anterograde and retrograde transport in the distal boutons with a mild bias towards retrograde moving vesicles (Figure 8D and 8F). In mutant animals, this bias was no longer visible and far fewer, if any, vesicles were observed leaving the distal bouton (Figure 8E and 8F). When we tracked individual vesicle movement, we found that their transport was not directionally oriented, but was sporadic and spontaneous, similar to movement ascribed to Brownian motion (Figure 8E). This loss of directionality might explain why the endosomes failed to leave the distal bouton in mutant animals and indicates a role for Vezatin in either attaching the cargo to dynein, or the attaching the dynein/cargo complex to microtubules following endocytosis.

Loss of Vezl does not affect microtubule formation in NMJs

To verify that the defect in transport was the result of cargo loading rather than a defect in the microtubule tracts themeselves, we examined microtubule structure using antibodies for the microtubule binding protein Futsch to make sure microtubule tracts were forming correctly in *vezl* mutants. We found that even the abnormally large distal boutons of mutant larvae still displayed typical Futsch staining and still contained Futsch "loops", which are indicative of a stable microtubule structure in mature boutons (Roos et al. 2000) (Figure 8G and 8I). Even the smaller satellite boutons showed diffuse Futsch staining which is similar to what in seen in smaller, less developed boutons in control animals (Figure 8H).

Additionally, super-resolution images showed that even boutons with intense HRP accumulation, Futsch staining appeared normal, indicating that membrane accumulation around the microtubules is not affecting their organization and structure (Figure 8H and 8J). Together the presence of Futsch in these distal boutons, and the rest of the NMJ, seems to indicate that the microtubule network is developed and is not the cause for disruption in transport seen in Vezl loss.

Human Vezatin is unable to rescue loss of Vezl in flies

We've identified a role for Vezatin-like in retrograde axonal transport, which would be a novel role for Vezatin in other species. Could mammalian Vezatin perform this function as well? While the amino acid sequence between fly and human Vezatin is poorly conserved (Figure 1G), there remains a strikingly similar predicted domain structure, in both composition and relative location (Figure 1H). We therefore tested whether this similarity in domain structure was sufficient to maintain a similar function, by testing if mammalian Vezatin is sufficient to prevent the swelling of NMJ terminal boutons by Vezl loss in fly. We generated a UAS-human Vezatin transgene and expressed it in the motorneurons of *vezl* mutant flies. While transgenic expression of fly Vezl fully rescued *vezl* loss (Figure 2), hVez showed no apparent signs of rescue in either NMJ size or distal bouton morphology (Figure 9B). To see if hVez was being expressed in a similar manner as Vezl, we tagged hVez with a Venus tag and tested its localization. While fly Vezl was enriched in distal boutons (Figure 3E), hVez expression was diffuse throughout the bouton and did not show distal enrichment (Figure 9A). These results indicate that human and fly Vezatin

proteins are not conserved well enough for hVez to be able replace Vezl in its function in flies, but it does not rule out the possibility that human Vezatin serves a similar function in human cells. Ultimately, Vezatin's potential role in axonal transport will have to be directly tested in vertebrates.

FUTURE EXPERIMENTS

Two questions remain in our present study: What is the molecular function of Vezl in retrograde transport, and is this function conserved in other Vezatin homologues? To address the first question, we generated a transgene expressing vezl with a terminal FLAG epitope that we can use to conduct binding and pull-down experiments. From these results we hope to identify potential binding partners of Vezl as well as test interactions between Vezl and dynein or dynein associated proteins.

For the second question, we established a collaboration with a lab that specializes in retrograde axonal transport in Zebrafish. Based on their preliminary findings, Zebrafish Vezatin (zVez) may also be required for retrograde transport of endosomes, but not other cargo, and *zvez* mutants had terminal axon swelling akin to fly. While hVez failed to rescue the loss of *vezL* in fly, this data indicates that Vezatin's role as a regulator of retrograde endosomal transport is conserved between species.

DISCUSSION

Fly Vezatin-like as a homologue to vertebrate Vezatin

In the present study, we identified a previously uncharacterized gene as being required for retrograde axonal transport. Simple BLAST searches failed to detect sequence similarity between CG7705 and proteins from non-Drosophilid species. To identify more distantly related proteins, we used Position-Specific Iterative (PSI)-BLAST. On the third iteration, PSI-BLAST identified CG7705 as having the closest similarity to the mammalian protein Vezatin. While amino acid sequence is poorly conserved between fly and vertebrates, the Vezatin proteins has a relatively conserved predicted domain structure consisting of an alphahelical transmembrane domain, a myosin binding "Vezatin" domain, and stretches in the C- and N- terminus containing low complexity regions.

A recent study of a distant Vezatin homologue in fungus, found that Vezatin was required tor initiation of retrograde transport of early endosomes through interactions with the adaptor protein, HookA (Yao et al. 2015). However, vertebrate Vezatin is not known to regulate the localization of presynaptic material or axonal transport. While such a function has yet to de directly tested (outside of our collaboration in zebrafish), Vezatin localizations at adherens junctions and its ability to bind to myosin and regulate cell motility could be early indications of a conserved role. Also, since Vezatin has been found to be expressed in multiple tissue types, it's possible that this role in transport is not specific to neurons and could be required in other cell types as well.

Model for Vezatin's role in retrograde axonal transport

Loss of Vezl resulted in terminal swellings, increased neuronal membrane accumulation and caused an increase in the presence of synaptic cargo in distal boutons. Through our searches trying to identify other similar mutants, we'd only identified one other instance that gave a similar phenotype, the mutation in the $p150^{Glued}$ subunit of the dynein/dynactin complex (Llyod et al. 2012). Lloyd et al. concluded that the $p150^{Glued}$ mutation resulted in a failure of dynactin to load back onto microtubules after they'd fallen off of microtubule ends, and accumulated at distal boutons. What then may be causing this accumulation and swelling in *vezl* animals? As with $p150^{Glued}$ mutants, *vezl* larvae were enriched for synaptic cargo at distal boutons, but the accumulation consisted only of endosomes and dense core vesicle, but not mitochondria, synaptic vesicles, or recycling endosomes. Together, this indicates that Vezl has cargo specificity towards cargo, and predominately affects those that undergo retrograde transport. In support of this, live imaging found that almost all transport seen in the axons was anterograde directed, and very few if any vesicles were observed moving retrogradely.

Further, while Lloyd et al. saw an accumulation of synaptic vesicle markers in distal tips, we did not (Figure 2A-D). This further sets apart Vezl from dynactin, showing a level of selectivity for cargo that was not seen in the $p150^{Glued}$ mutants. While we saw an increase in dense core vesicles, the most striking change was in the accumulation of endosomes and Tkv-mCherry positive vesicles (Figure 4G-M, Figure 5C-D). While the mechanism by which Vezl might act is presently unclear, we

support a possible model where Vezatin functions in distal boutons, and facilitates the binding of endosome to motor proteins.

In support of this, we noticed a large population of endosomes that were stationary in the axons of *vezl* mutants (Figure 6A and 7A). We believe these may result to *vezl* loss destabilizing the connection between cargo and motor protein. Previous studies have shown that loss of binding stability between motor proteins and their cargo reduces processivity of the motors which can result in stalled or stopped cargo (Hurd and Saxton, 1996), similar to what we'd seen in *vezl* animals. Ultimately, identifying binding partners of Vezl will help elucidate its function. Additionally, while we've found partial specificity towards the BMP signaling pathways, determining whether Vezl is specific to the BMP pathway, or similarly affects other signaling pathways will be of great interest in both fly and vertebrates.

Vezatin's role in BMP signaling

We found that BMP signaling pathway markers also accumulated in distal boutons of *vezl* mutants. In *Drosophila*, BMP signaling relies on retrograde transport of BMP receptors within Rab5, then Rab7, labeled endosomes back to the cell body (Smith et al. 2012). Based on our live imaging results, these signaling endosomes appear trapped in distal boutons of *vezl* animals, and BMP signaling is severely impaired. In support of this, loss of BMP signaling has been shown to result in an overall decreased NMJ size (Smith et al. 2012) similar to what we see with *vezl* loss (Figure 2B and 3B). Additionally, upregulating the BMP signaling pathway by either

increasing BMP expression or increasing endocytosis results in increased NMJ size. We also see a gain of function phenotype caused by overexpression of Vezl, and hypothesize that Vezl may also be resulting in increase endocytosis through the rapid loading and transport of BMP endosomes back to the nucleus. Future experiments will have to directly test whether Vezl is affecting BMP levels in the nucleus, but current similarities in phenotypes strongly indicates a direct interaction between Vezl and BMP signaling.

CONCLUSIONS

Here I describe two important findings about synapse development:

In Chapter II, I studied an established synaptic protein, Syd-1, and detailed the role of its GAP domain whose function had previously been a point of contention in the field. By abolishing Syd-1's GAP activity in an otherwise functional transgene, I was able to test the requirement of Syd-1's GAP activity in its previously described functions. While not all of Syd-1's functions required GAP activity, the ability to cluster BRP and establish functional active zones was. I then went on to show that Syd-1 genetically interacts with the Rho GTPase Rac1 *in vivo*. This interaction could provide a potential link as to how active zone establishment and synaptic protein recruitment can further promote neuron growth and increased synapse formation. Overall these findings help further understand the role of active zone proteins in synapse development and also introduces and alternative interpretation of how Syd-1 may be functioning in vertebrates.

The study in Chapter III characterized a new gene, Vezatin-like, and identified a potential mechanism involved in axonal transport. I identified a novel phenotype caused by *vezl* loss that was the result of defects in axonal transport and resulted in synaptic cargo to accumulate in distal boutons. Through live imaging, I was able to confirm that cargo was accumulating due to a failure of endosomes to undergo retrograde transport. I concluded that Vezl is either required in the attachment of specific cargo to the molecular motor dynein or in the connection of molecular motor to the microtubules. Based off of Vezatin's predicted domain structure that is shared between species, as well as preliminary data from a collaborator working in zebrafish, we believe this function is conserved in higher organisms as well.

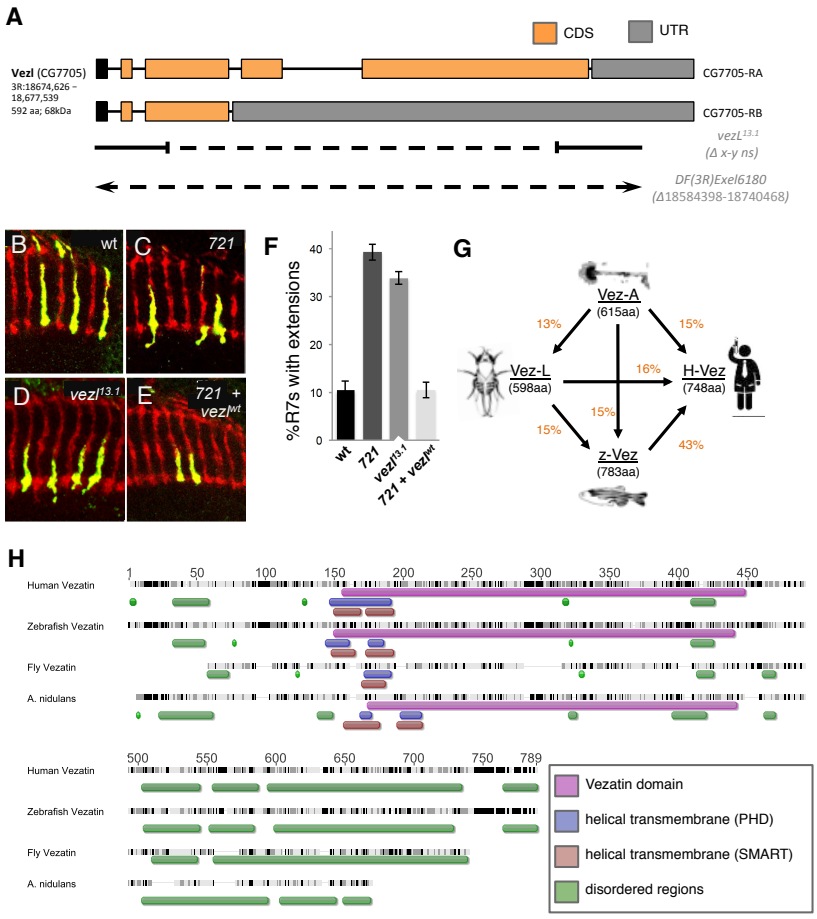

Figure 1. CG7705/Vezatin-like (Vezl) is required for normal photoreceptor axon terminal morphology.
(A) Genomic structure of the previously uncharacterized gene *vezl* (*CG7705*) showing the exons contained in *vezl* mRNAs and the breakpoints of the small *vezl*$^{13.1}$ deletion. The large deficiency Df(3R)Exel6180 completely removes *vezl* together with 23 additional genes. (B) wild-type *Drosophila* R7 photoreceptors terminate in within the M6 layer of medulla (homozygous wt R7s are green, and heterozygous wt R7s are red). (C) The EMS-generated *721* mutation causes R7s to extend blobby projections past their target layer (homozygous *721* mutant R7s are green, and heterozygous R7s are red). (D) Deletion of *vezl* phenocopies the *721* mutant defect. (E) Expression of a *vezl* cDNA fully rescues both *721* and *vezl*$^{13.1}$. (F)Quantification of the R7 defect.(F) Sequence similarity between Vezatin family proteins. Values in orange represent % identical sequence between animals. Values in purple represent % conserved sequence shared between animals. (G) Sequence alignment of Vezatin family proteins. Black regions indicate conserved sequence and dark grey indicates >80% conserved sequence (Clustal W). Purple bars indicate myosin binding "Vezatin" domain. Blue (PHD) and Red (SMART) indicate predicted helical transmembrane domain predicted by two different algorithms. Orange indicates low complexity regions.

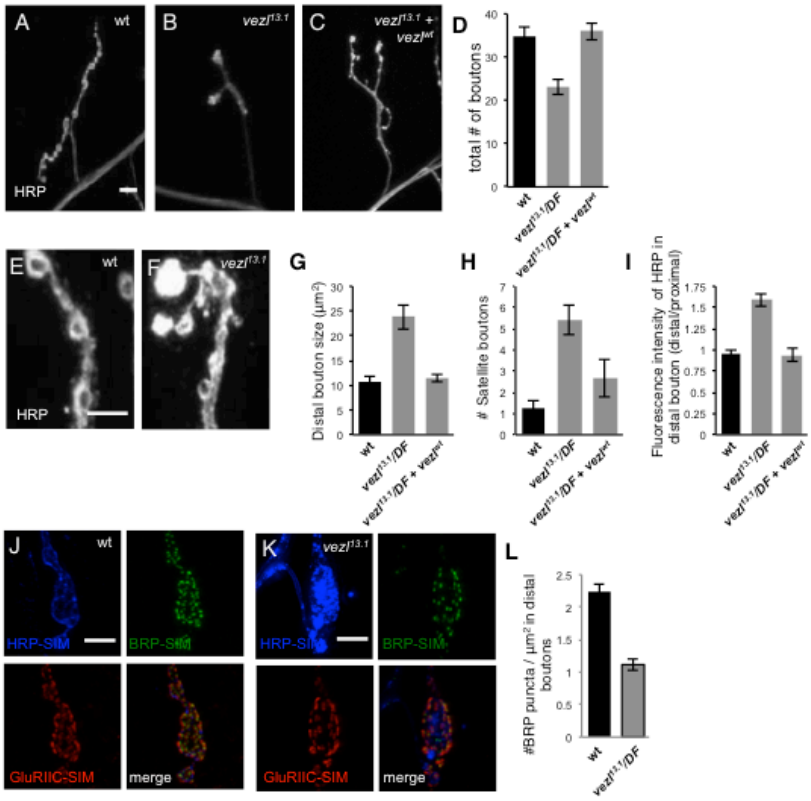

Figure 2. Loss of Vezl results in defects in larval neuromuscular junction development and distal bouton morphology.
(A) wild-type *Drosophila* neuromuscular junction (NMJ) at muscle 4. *(B) vezl$^{13.1}$/Df(3R)Exel6180* mutants have smaller NMJs than wt animals. (C) Expression of a *vezl* cDNA in motorneurons fully restores NMJs to normal size in *vezl$^{13.1}$/Df(3R)Exel6180* mutants. (D) Quantification of NMJ size. (E) Zoom in of wild-type boutons labeled with HRP. In wild-type, HRP labels presynaptic membrane and therefore outlines each bouton; the distal bouton (top) is similar in size to more proximal boutons. (F) Zoom in on *vezl$^{13.1}$/Df(3R)Exel6180* mutant boutons. The distal bouton (top left) is enlarged, contains significantly increased HRP staining, and has "satellite boutons" branching from it. (G) Quantification of terminal bouton size. (H) Quantification of distal satellite boutons. (I) Quantification of HRP staining in distal bouton as compared to proximal boutons as the same NMJ. (J) Structured illumination microscopy (SIM) image of a distal bouton in wild-type showing active zone (anti-Brp (green)) and postsynaptic density (anti-GluIIC (a glutamate receptor (red))) components in apposition. (K) SIM image of a distal bouton in a *vezl$^{13.1}$/Df(3R)Exel6180* mutant animal showing the same apposition of pre- and post-synaptic components but at decreased density. Barren areas appear to correlate with areas having increased anti-HRP staining (merge panel has reduced HRP intensity to show detail). (L) Quantification of anti-Brp puncta density in distal boutons.

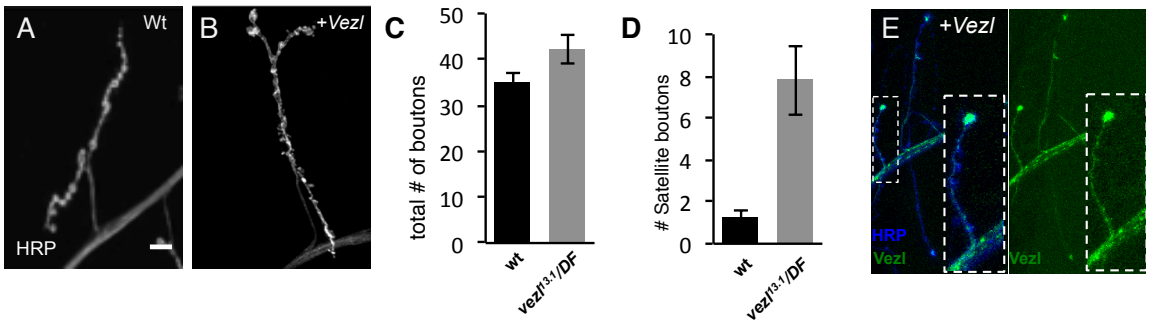

Figure 3. Vezl promotes NMJ development and localizes along axons and is enriched in distal boutons.
(A) wild-type *Drosophila* neuromuscular junction (NMJ) at muscle 4. (B)Expression of *vezl* in motorneurons causes a gain of function phenotype resulting in creased NMJ size and satellite bouton number compared to wild-type. (C) Quantification of NMJ growth phenotype. (D) Quantification of satellite boutons. (E) Vezl-Venus expressed in motorneurons of wild-type animals localizes to the interior of axons and proximal boutons and is enriched within distal boutons.

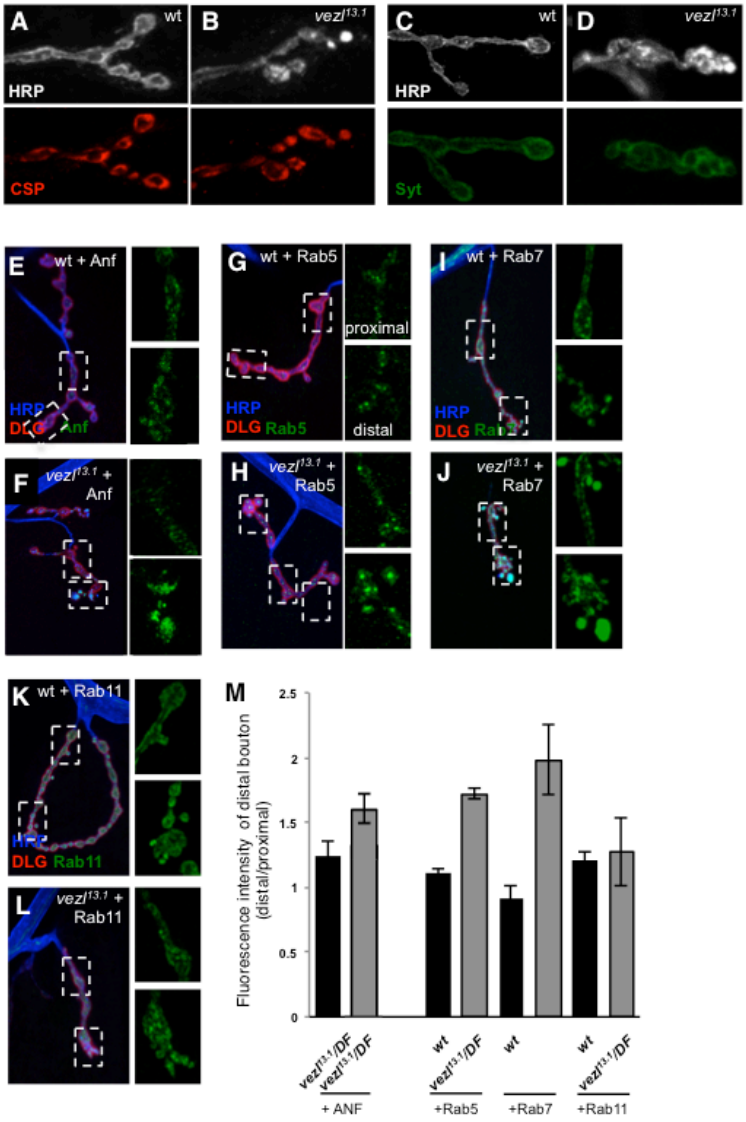

Figure 4. Distal NMJ boutons in *vezl* mutants have normal-looking synaptic vesicle distribution but abnormal dense corve vesicles and endosomes. (A)Anti-cystein string protein (Csp) staining in wild-type animals uniformly outlines wild-type NMJ boutons. (B)Anti-Csp staining in *vezl* NMJs appears normal and is neither enriched nor decreased in distal boutons. (C)Anti-Synaptotagmin (Syt) staining in wild-type animals uniformly outlines wild-type NMJ boutons. (D) Anti-Syt staining in *vezl* NMJs appears normal and is neither enriched nor decreased in distal boutons, suggesting that synaptic vesicle transport and recruitment are unaffected by loss of Vezl. (E) Expression of the dense core vesicle marker ANF-GFP in motorneurons of wild-type animals localizes to puncta that are uniformly distributed among proximal and distal boutons. (F) The distribution of Anf-GFP is increased in the distal boutons of *vezl* mutants than in more proximal bouotns. (G) Expression of the early endosome marker Rab5-GFP in motorneurons of wild-type animals localizes to puncta that are uniformly distributed among proximal and

distal boutons. (H) Rab5-GFP expressed in motorneurons of *vezl$^{13.1}$/Df(3R)Exel6180* mutants clusters more densely and at greater levels in distal boutons than in more proximal boutons. (I) Expression of the early-late endosome marker Rab7-GFP in motorneurons of wild-type animals localizes to puncta that are uniformly distributed among proximal and distal boutons. (J) Rab7-GFP expressed in motorneurons of *vezl$^{13.1}$/Df(3R)Exel6180* mutants is also enriched in distal and satellite boutons. (K) Expression of the recycling endosome marker Rab11-GFP in motorneurons of wild-type animals localizes to puncta that are uniformly distributed among proximal and distal boutons. (L) Rab11-GFP expression and localization appears unaffected by loss of *vezl*, showing no enrichment in distal boutons. (M) Quantification of reporter intensity in distal boutons compared to more proximal boutons.

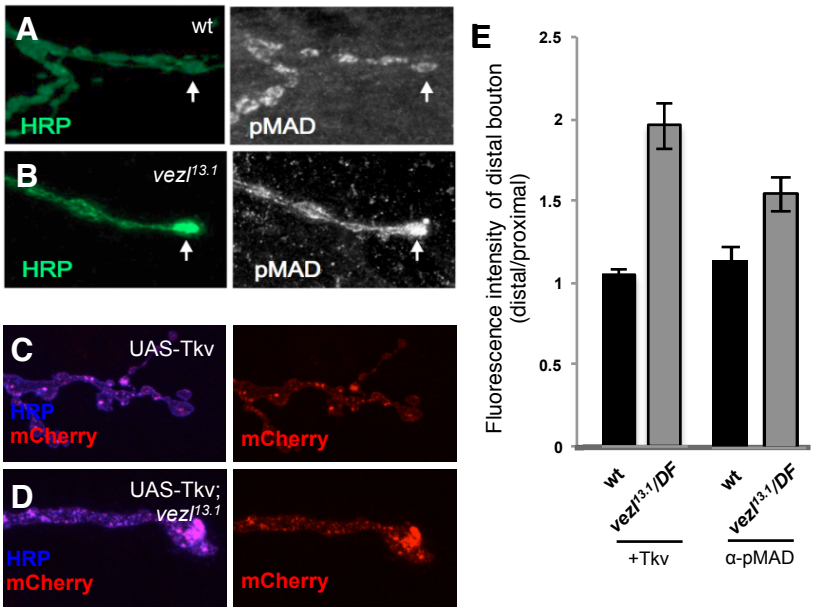

Figure 5. Retrograde BMP signaling is affected in *vezl* mutants.
(A) In wild-type, phosphorylated Mad (pMad), the downstream target of BMP signaling in motorneurons, localizes to puncta within both proximal and distal boutons. (B) Anti-pMad staining is enriched in distal boutons in *vezl*$^{13.1}$*/Df(3R)Exel6180* mutants. (C) In wild-type, tagged BMP type I receptor marker Tkv-mCherry expressed in motorneurons localizes to puncta that are uniformly distributed among proximal and distal boutons. (D) In *vezl*$^{13.1}$*/Df(3R)Exel6180* mutants, Tkv-mCherry expressed in motorneurons is enriched in distal boutons. (E) Quantification of pMad staining and Tkv-mCherry levels .

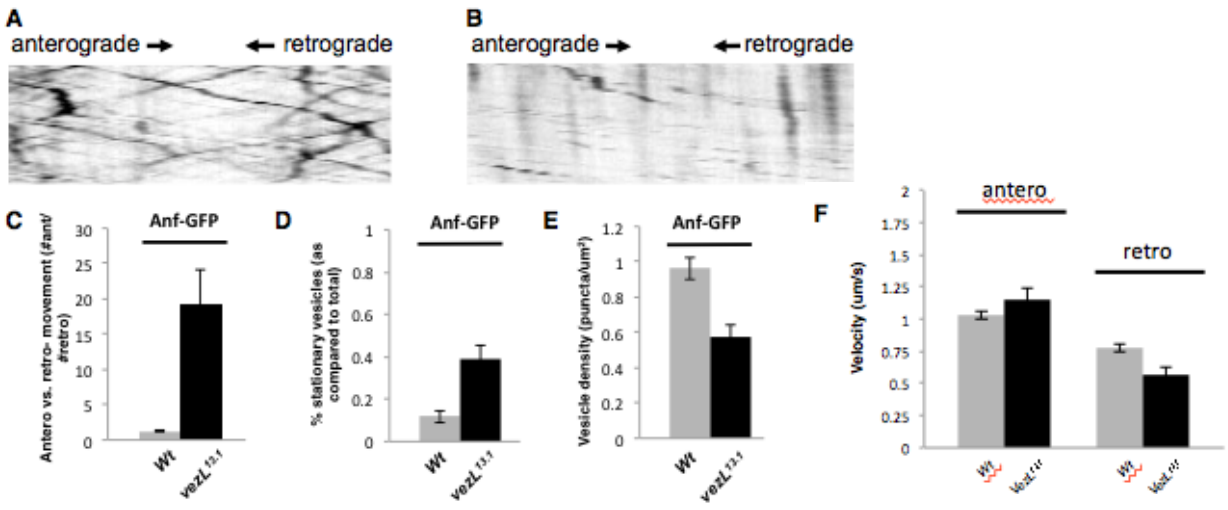

Figure 6. Dense core vesicle transport is disrupted in *vezl* mutants.
(A) Representative kymograph of ANF-GFP transport in wild-type animals. x-axis represents distance and y-axis represents time. Lines sloping down from left to right indicate a vesicle undergoing retrograde transport. Lines sloping up from left to right indicate vesicles undergoing retrograde transport. Vertical lines are nonmoving vesicles. (B) Representative kymograph of ANF-GFP transport in *vezl* mutants. There were fewer moving, and more non-moving vesicles observed in mutants. Retrograde moving vesicles were virtually absent. (C) Ratio of anterograde to retrograde moving vesicles. (D) Percentage of stationary vesicles observed. (E) Overall vesicle density within the axon. (F) Velocities of moving vesicles.

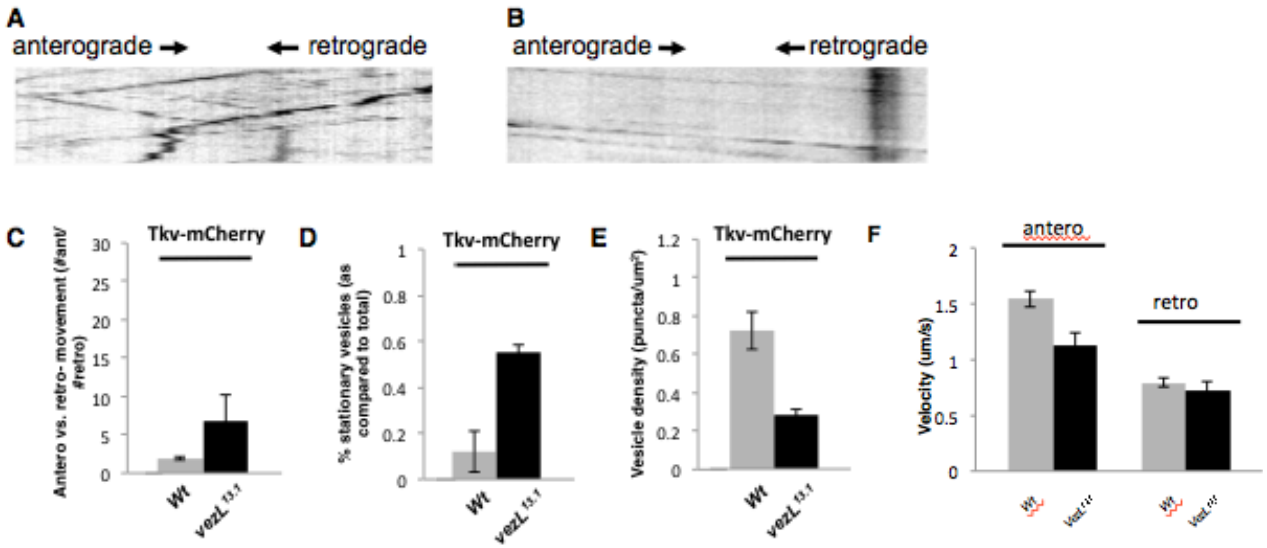

Figure 7. Transport of BMP signaling molecules are also disrupted in *vezl* mutants.

(A) Representative kymograph of Tkv-mCherry transport in wild-type animals. x-axis represents distance and y-axis represents time. Lines sloping down from left to right indicate a vesicle undergoing retrograde transport. Lines sloping up from left to right indicate vesicles undergoing retrograde transport. Vertical lines are nonmoving vesicles. (B) Representative kymograph of Tkv-mCherry transport in *vezl* mutants. There were fewer moving, and more non-moving vesicles observed in mutants. Retrograde moving vesicles were virtually absent. (C) Ratio of anterograde to retrograde moving vesicles. (D) Percentage of stationary vesicles observed. (E) Overall vesicle density within the axon. (F) Velocities of moving vesicles.

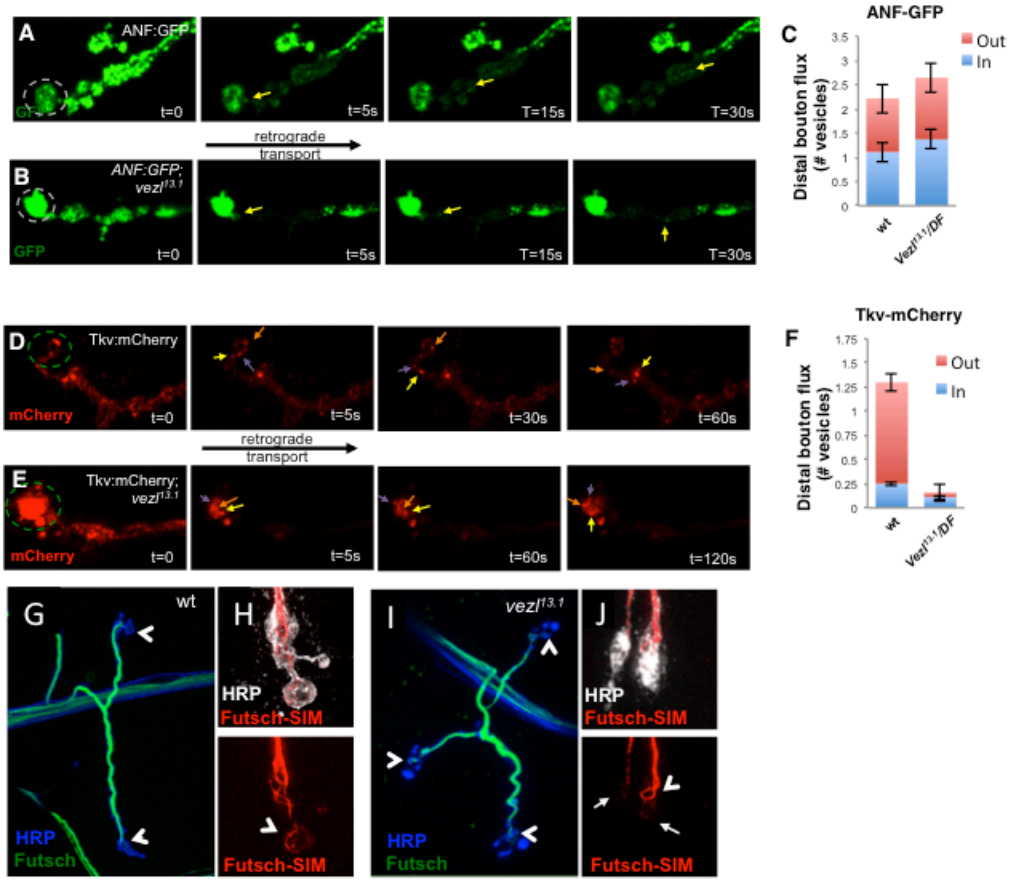

Figure 8. Retrograde transport of endosomes is disrupted in the distal boutons of *vezl* mutants.

(A) Expression of ANF-GFP in motorneurons of a live wild-type 3rd instar larva. Regions adjacent to the distal bouton were photobleached and retrograde movement of ANF-GFP puncta out of the distal bouton was monitored, as was anterograde movement into the bleached region. (B) Movement of ANF-GFP puncta was normal in in *vezl*$^{13.1}$*/Df(3R)Exel6180* mutants. (C) Quantification of movement of ANF-GFP stained vesicles in distal boutons as measured by live imaging. (D) Expression of Tkv-mCherry in motorneurons of a live wild-type 3rd instar larva. Regions adjacent to the distal bouton were photobleached and retrograde movement of Tkv-mCherry out of the distal bouton was monitored, as was anterograde movement into the bleached region. (E) Tkv-mCherry puncta in *vezl*$^{13.1}$*/Df(3R)Exel6180* mutants failed to exit the distal bouton and instead circulated around in an unorganized fashion (note the extended recording time compared to wild-type). (F) Quantification of movement of Tkv-mCherry vesicles in distal boutons as measured by live imaging. (G) Microtubule tracks stained by anti-Futsch/MAP1B. (H) SIM images show that Futsch is present throughout wt boutons and forms stabilized "loops" in terminal boutons (arrowheads). (I) Distal boutons in *vezl*$^{13.1}$*/Df(3R)Exel6180* mutants still contain Futsch loops (arrowheads), although satellite boutons do not. (J) Super resolution shows that regions of the bouton that have elevated HRP levels, lack organized Futsch staining (arrows).

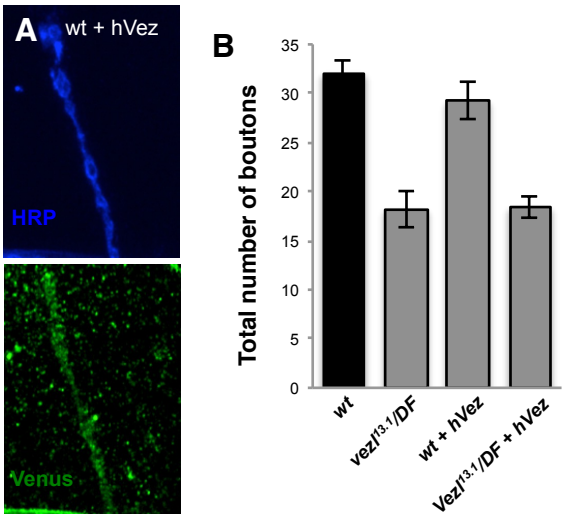

Figure 9. Expression of a human Vezatin (hVez) transgene is unable to properly localize and cannot rescue loss of *vezl*.
(A) Expression of human vezatin (hVez-Venus) in wild-type motorneurons. Staining for anti-Venus showed diffuse, rather than confined, staining that is not enriched in distal boutons. (B) Quantification of hVez's ability to rescue loss of Vezl.

APPENDIX A

SUPPLEMENTAL MATERIAL FOR CHAPTER II

SUPPLEMENTAL FIGURES

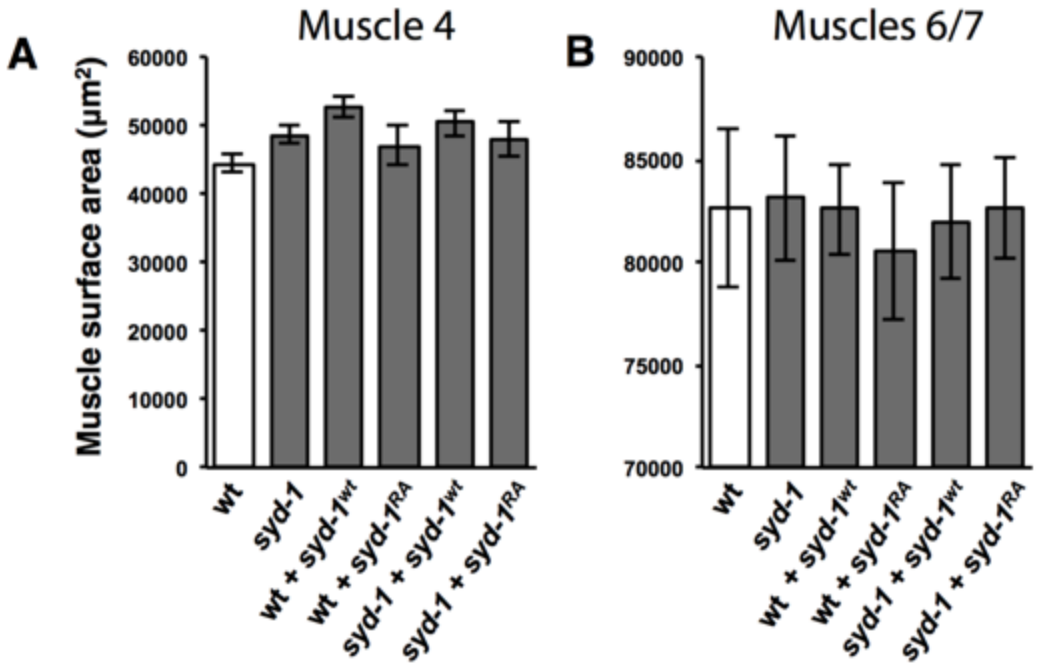

Figure S1. No differences in muscle size among the genotypes tested.
Because stochastic variation in body size among fly larvae causes slight variations in NMJ size, it is standard to report bouton number per muscle area (Schuster et al. 1996). We here present a selection of the measurements of muscle area that were used to normalize the corresponding counts of bouton number in order to note that we observed no significant differences in muscle area. (A) Quantification of the surface area of muscle 4 in abdominal segment 3. There was no significant difference among the genotypes (one-way ANOVA: $F(5,58)=1.84$, $p=0.12$). (B) Quantification of the surface area of muscles 6/7 in abdominal segment 3. There was no significant difference among the genotypes (one-way ANOVA: $F(5,84)=0.077$, $p=0.99$)

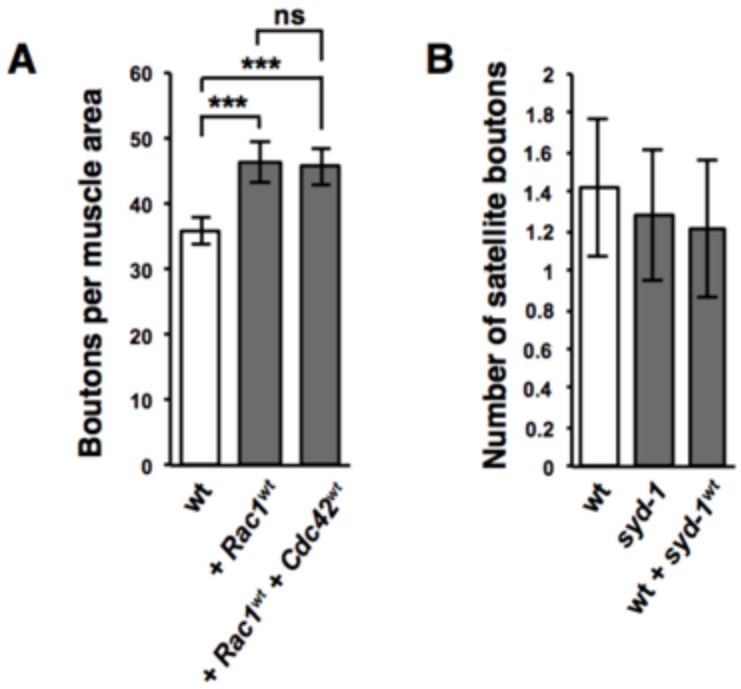

Figure S2. Gain or loss of Syd-1 does not increase satellite bouton number, and Cdc42 overexpression is not sufficient to prevent Rac1 from increasing NMJ bouton number.

(A) Quantification of the number of boutons on muscle 4 in abdominal segment 3 per muscle area. As expected, overexpressing Rac1wt in the motorneurons of wild-type animals increases bouton number (BG380-Gal4, UAS-Rac1wt: 46.2±2.4, n=11) compared to wild-type (BG380-Gal4 alone: 35.8±2.0, n=12, p=0.004). Coexpression of Cdc42wt with Rac1wt (BG380-Gal4, UAS-Rac1wt, UAS-Cdc42wt::45.8±2.8, n=10) does not cause a significant decrease in this number (p=0.45 compared to Rac1wt alone). (B) Quantification of the number of satellite boutons on muscle 4 in abdominal segment 3. Satellite boutons are smaller boutons that bud off a larger, main bouton and are otherwise not connected to the linear chain of main boutons (e.g. Nahm et al. 2014). Overexpressing wild-type Syd-1 in motorneurons (BG380-Gal4, UAS-syd-1wt: 1.2±0.3, n=14) or entirely eliminating Syd-1 (syd-1CD/syd-1w46: 1.3±0.3, n=18) does not increase satellite bouton number compared to wild-type (BG380-Gal4 alone: 1.4.8±0.4, n=19, p=0.76 and p=0.68 respectively).

APPENDIX B

SUPPLEMENTAL MATERIAL FOR CHAPTER III

SUPPLEMENTAL FIGURES

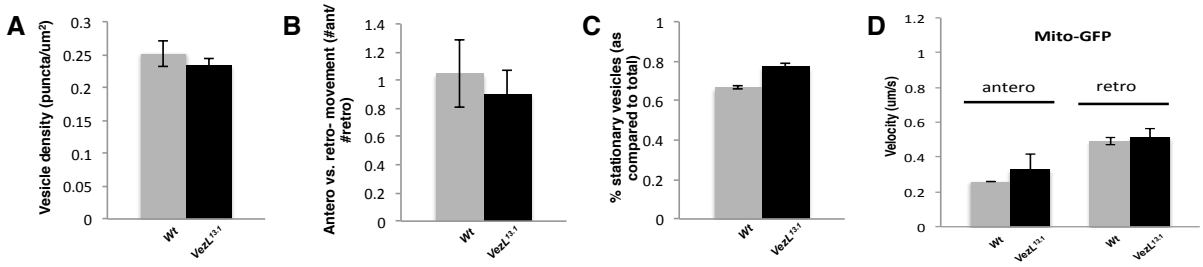

Figure S1. Live transport of mitochondria is unaffected in *vezl* mutants.
(A) Ratio of anterograde to retrograde moving mitochondria. (B) Percentage of stationary mitochondria observed. (C) Overall mitochondria density within the axon. (D) Velocities of moving mitochondria.

REFERENCES CITED

CHAPTER I

Cioni, J.M., Koppers, M., and Holt C.E. (2018) Molecular control of local translation in axon development and maintenance. Curr. Op. Neurobiology. 51, 86-94

Maritzen, T. and Haucke, V. (2018) Coupling of exocytosis and endocytosis at the presynaptic active zone. Neuroscience Research. 127, 45-52

Perlson E, Maday S, Fu MM, Moughamian AJ, Holzbaur EL (2010) Retrograde axonal transport: pathways to cell death? Trends Neurosc 33:335-344.

Torres, V. I., and Inestros, N. C. (2017) Vertebrate presynaptic active zone assembly: A Role accomplished by diverse molecular and cellular mechanisms. Molecular Neurobiology. 1-16

CHAPTER II

Ball, R. W., M. Warren-Paquin, K. Tsurudome, E. H. Liao, F. Elazzouzi *et al.*, 2010 Retrograde BMP signaling controls synaptic growth at the NMJ by regulating Trio expression in motor neurons. Neuron 66: 536-549.

Budnik, V., Y. H. Koh, B. Guan, B. Hartmann, C. Hough *et al.*, 1996 Regulation of synapse structure and function by the *Drosophila* tumor suppressor gene Dlg. Neuron 17: 627-640.

Chia, P. H., M. R. Patel, and K. Shen, 2012 NAB-1 instructs synapse assembly by linking adhesion molecules and F-actin to active zone proteins. Nat. Neurosci. 15: 234-242.

Chia, P. H., P. Li, and K. Shen, 2013 Cellular and molecular mechanisms underlying presynapse formation. J. Cell Biol. 203: 11-22.

Dai, Y., H. Taru, S. L. Deken, B. Grill, B. Ackley, *et al.*, 2006 SYD-2 Liprin-alpha organizes presynaptic active zone formation through ELKS. Nat. Neurosci. 9: 1479-1487.

Emery, P., 2007 Protein extraction from *Drosophila heads*. Methods Mol. Biol. 362: 375-377.

Fritz, R. D. and O. Pertz, 2016 The dynamics of spatio-temporal Rho GTPase signaling: formation of signaling patterns. F1000Res 5(F1000 Faculty Rev): 749.

Garcia-Mata, R., K. Wennerberg, W. T. Arthur, N. K. Noren, S. M. Ellerbroek, *et al.*, 2006 Analysis of activated GAPs and GEFs in cell lysates. Methods Enzymol. 406: 425-437.

Graham, D. L., J.F. Eccleston, and P.N. Lowe, 1999 The conserved arginine in Rho-GTPase-activating protein is essential for efficient catalysis but not for complex formation with Rho.GDP and aluminum fluoride. Biochemistry 38: 985–991.

Hakeda-Suzuki, S., J. Ng, J. Tzu, G. Dietzl, Y. Sun, *et al.*, 2002 Rac function and regulation during Drosophila development. Nature 416: 438-442.

Hallam, S. J., A. Goncharov, J. McEwen, R. Baran, and Y. Jin, 2002 SYD-1, a presynaptic protein with PDZ, C2, and RhoGAP-like domains, specifies axon identity in *C. elegans*. Nat. Neurosci. 5: 1137-1146.

Holbrook, S., J. K. Finley, E. L. Lyons, and T. G. Herman, 2012 Loss of *syd-1* from R7 neurons disrupts two distinct phases of presynaptic development. J. Neurosci. 32: 18101-18111.

Kittel, R. J., C. Wichmann, T. M. Rasse, W. Fouquet, M. Schmidt, *et al.*, 2006 Bruchpilot promotes active zone assembly, Ca^{2+} channel clustering, and vesicle release. Science 312: 1051-1054.

Li, J., J. Ashley, V. Budnik, and M. A. Bhat, 2007 Crucial role of *Drosophila neurexin* in proper active zone apposition to postsynaptic densities, synaptic growth, and synaptic transmission. Neuron 55: 741-755.

Luo, L., Y. J. Liao, L. Y. Jan, and Y. N. Jan, 1994 Distinct morphogenetic functions of similar small GTPases: *Drosophila* Drac1 is involved in axonal outgrowth and myoblast fusion. Genes Dev. 8: 1787-1802.

Melom, J. E. and J. T. Littleton, 2011 Synapse development in health and disease. Curr. Opin. Genet. Dev. 21: 256-261.

Nahm, M., S. Kim, S. K. Paik, M. Lee, S. Lee, *et al.*, 2010 dCIP4 (*Drosophila* Cdc42-interacting protein 4) restrains synaptic growth by inhibiting the secretion of the retrograde Glass bottom boat signal. J Neurosci. 30: 8138-8150.

Nelson, J. N., A. K. Stavoe, D. A. Colon-Ramos, 2013 The actin cytoskeleton in presynaptic assembly. Cell Adh. Migr. 7: 379-387.

Owald, D., W. Fouquet, M. Schmidt, C. Wichmann, S. Mertel, *et al.*, 2010 A Syd-1 homologue regulates pre- and postsynaptic maturation in *Drosophila*. J. Cell Biol. 188: 563-579.

Owald, D., O. Khorramshahi, V. K. Gupta, D. Banovic, H. Depner, *et al.*, 2012 Cooperation of Syd-1 with Neurexin synchronizes pre- with postsynaptic assembly. Nat. Neurosci. 15: 1219-1226.

Parrini, M.C. and J. Camonis, 2011 Cell motility: the necessity of Rac1 GDP/GTP flux. Commun. Integr. Biol. 4: 772-774.

Patel, M. R., E. K. Lehrman, V. Y. Poon, J. G. Crump, M. Zhen, *et al.*, 2006 Hierarchical assembly of presynaptic components in defined *C. elegans* synapses. Nat. Neurosci. 9: 1488-1498.

Rodal, A. A., R. N. Motola-Barnes, and J. T. Littleton, 2008 Nervous wreck and Cdc42 cooperate to regulate endocytic actin assembly during synaptic growth. J. Neurosci. 28: 8316-8325.

Rossman, K. L., C. J. Der, and J. Sondek, 2005 GEF means go: turning on Rho GTPases with guanine nucleotide-exchange factors. Nat. Rev. Mol. Cell Biol. 6: 167-180.

Scheffzek, K. and M. R. Ahmadian, 2005 GTPase activating proteins: structural and functional insights 18 years after discovery. Cell. Mol. Life Sci. 62: 3014-3038.

Schindelin, J., I. Arganda-Carreras, E. Frise, V. Kaynig, M. Longair, *et al.*, 2012 Fiji: an open-source platform for biological-image analysis. Nat. Methods 9: 676-682.

Schuster, C. M., G. W. Davis, R. D. Fetter, C. S. Goodman, 1996 Genetic dissection of structural and functional components of synaptic plasticity. I. Fasciclin II controls synaptic stabilization and growth. Neuron 17: 641-654.

Sharif, B., and A. S. Maddox, 2012 Wound healing: GTPases flux their muscles. Dev. Cell 23: 236-238.

Stankiewicz, T. R. and D. A. Linseman, 2014 Rho family GTPases: key players in neuronal development, neuronal survival, and neurodegeneration. Front. Cell. Neurosci. 8: 314.

Symons, M. and J. Settleman, 2000 Rho family GTPases: more than simple switches. Trends Cell Biol. 10: 415-419.

Tcherkezian, J. and N. Lamarche-Vane, 2007 Current knowledge of the large RhoGAP family of proteins. Biol. Cell 99: 67-86.

Tolias, K.F., J. G. Duman, and K. Um, 2011 Control of synapse development and plasticity by Rho GTPase regulatory proteins. Prog. Neurobiol. 94: 133-148.

Wentzel, C., J. E. Sommer, R. Nair, A. Stiefvater, J. B. Sibarita, *et al.*, 2013 mSYD1A, a mammalian synapse-defective-1 protein, regulates synaptogenic signaling and vesicle docking. Neuron 78: 1012-1023.

Xu, Y., H. Taru, Y. Jin, and C. C. Quinn, 2015 SYD-1C, UNC-40 (DCC) and SAX-3 (Robo) function interdependently to promote axon guidance by regulating the MIG-2 GTPase. PLoS Genet. 11: e1005185.

Zhang, B., J. Chernoff, Y. Zheng, 1998 Interaction of Rac1 with GTPase-activating proteins and putative effectors: a comparison with Cdc42 and RhoA. J. Biol. Chem. 273: 8776-8782.

Chapter III

Ayloo, S., Lazarus, J. E., Dodda, A., Tokito, M., Ostap, E. M., and Holzbaur, E. L. (2014) Dynactin functions as both a dynamic tether and brake during dynein-driven motility. Nat. Commun. 5, 4807

Ball, RW., Warren-Paquin , M., Tsurudome , K., EH Liao F Elazzouzi C Cavanagh BS An TT Wang JH White AP Haghighi (2010) Retrograde BMP signaling controls synaptic growth at the NMJ by regulating trio expression in motor neurons. Neuron 66:536–549.

Bayat V, Jaiswal M, Bellen HJ (2011) The BMP signaling pathway at the Drosophila neuromuscular junction and its links to neurodegenerative diseases. Curr Opin Neurobiol 21:182-188.

Bucci, C., Alifano, P., and Cogli, L. (2014) The role of Rab proteins in neuronal cells and in trafficking of neurotrophin receptos. Membranes. 4, 642-677

Chowdhury, S., Ketcham, S. A., Schroer, T. A., and Lander, G. C. (2015) Structural organization of the dynein-dynactin complex bound to microtubules. Nat. Struct. Mol. Biol. 22, 345–347

Cioni, J.M., Koppers, M., and Holt C.E. (2018) Molecular control of local translation in axon development and maintenance. Curr. Op. Neurobiology. 51, 86-94

Holleran, E. A., Ligon, L. A., Tokito, M., Stankewich, M. C., Morrow, J. S., and Holzbaur, E. L. (2001) βIII spectrin binds to the Arp1 subunit of dynactin. J. Biol. Chem. 276, 36598–36605

Hurd, D.D., Saxton, W.M. (1996) Kinesin mutations cause motor neuron disease phenotypes by disrupting fast axonal transport in Drosophila. Genetics. 144:1075-1085

Karki, S., and Holzbaur, E. L. (1995) Affinity chromatography demonstrates a direct binding between cytoplasmic dynein and the dynactin complex. J. Biol. Chem. 270, 28806–28811

Lloyd TE, Machamer J, O'Hara K, Kim JH, Collins SE, Wong MY, Sahin B, Imlach W, Yang Y, Levitan ES, McCabe BD, Kolodkin AL (2012) The p150(Glued) CAP-Gly domain regulates initiation of retrograde transport at synaptic termini. Neuron 74:344-360.

Maday S, Twelvetrees AE, Moughamian AJ, Holzbaur EL (2014) Axonal transport: cargo-specific mechanisms of motility and regulation. Neuron 84:292-309.

Moughamian, A. J., and Holzbaur, E. L. (2012) Dynactin is required for transport initiation from the distal axon. Neuron 74, 331–343

Muresan, V., Stankewich, M. C., Steffen, W., Morrow, J. S., Holzbaur, E. L., and Schnapp, B. J. (2001) Dynactin-dependent, dynein-driven vesicle transport in the absence of membrane proteins: a role for spectrin and acidic phospholipids. Mol. Cell 7, 173–183

Olenick, M., Tokito, T., Boczkowska, M., Dominques, R., and Holzbaur, E. (2018) Hook Adaptors Induce Unidirectional Processive Motillity by Enhancing the Dynein-Dynactin Interaction. J. Bio. Cehm. 291, 18239-18251

Perlson E, Maday S, Fu MM, Moughamian AJ, Holzbaur EL (2010) Retrograde axonal transport: pathways to cell death? Trends Neurosc 33:335-344.

Reck-Peterson, S.L, Redwine, W.B., Vale, R. D., and Carter, A.C. (2018) The cytoplasminc dynein transport machinery and its many cargoes. Nature reviews Molecular Cell Biology,

Rao S, Lang C, Levitan ES, Deitcher DL (2001) Visualization of neuropeptide expression, transport, and exocytosis in Drosophila melanogaster. J Neurobiol 49:159–172.

Roos J., Hummel T., Ng C., and Davis GW. (2000) Drosophila Futsch regulates synaptic microtubule organization and is necessary for synaptic growth. Neuron. 26:371-382

Roy S, Huang H, Liu S, Kornberg TB. Cytoneme-mediated contact-dependent transport of the Drosophila decapentaplegic signaling protein. Science. 2014;343:1244624.

Smith, G.M., and Gallo, G. (2017) The role of Mitochondria in axon development and repair. Dev. Neurobiology. 78:221-237

Smith RB, Machamer JB, Kim NC, Hays TS, Marqués G (2012) Relay of retrograde synaptogenic signals through axonal transport of BMP receptors. J Cell Sci 125(Pt 16):3752-3764.

Spinner MA, Walla DA, Herman TG. (2018) Drosophila Syd-1 Has RhoGAP Activity That Is Required for Presynaptic Clustering of Bruchpilot/ELKS but Not Neurexin-1. Genetics. 208:705-716

Torres, V. I., and Inestros, N. C. (2017) Vertebrate presynaptic active zone assembly: A Role accomplished by diverse molecular and cellular mechanisms. Molecular Neurobiology. 1-16

Urnavicius, L., Zhang, K., Diamant, A. G., Motz, C., Schlager, M. A., Yu, M., Patel, N. A., Robinson, C. V., and Carter, A. P. (2015) The structure of the dynactin complex and its interaction with dynein. Science 347, 1441–1446

Vaughan, K. T., and Vallee, R. B. (1995) Cytoplasmic dynein binds dynactin through a direct interaction between the intermediate chains and p150Glued. J. Cell Biol. 131, 1507–1516

Wucherpfennig T, Wilsch-Brauninger M, Gonzalez-Gaitan MJ (2003) Role of Drosophila Rab5 during endosomal trafficking at the synapse and evoked neurotransmitter release. Cell Biol 161:609–624.

Yao X, Arst HN Jr, Wang X, Xiang X (2015) Discovery of a vezatin-like protein for dynein-mediated early endosome transport. Mol Biol Cell 26:3816-3827.

Yeh, T.-Y., Quintyne, N. J., Scipioni, B. R., Eckley, D. M., and Schroer, T. A. (2012) Dynactin's pointed-end complex is a cargo-targeting module. Mol. Biol. Cell 23, 3827–3837

Zhang, J., Yao, X., Fischer, L., Abenza, J. F., Peñalva, M. A., and Xiang, X. (2011) The p25 subunit of the dynactin complex is required for dynein: early endosome interaction. J. Cell Biol. 193, 1245–1255

Zhang, J., Qiu, R., Arst, H. N., Jr.., Peñalva, M. A., and Xiang, X. (2014) HookA is a novel dynein-early endosome linker critical for cargo movement in vivo. J. Cell Biol. 204, 1009–1026